October 2021

Metabolic Modeling of Bacterial Co-cultures for CO-to-Butyrate Conversion in Bubble Column Bioreactors

Naresh Kandlapalli
University of Massachusetts Amherst

Metabolic Modeling of Bacterial Co-cultures for CO-to-Butyrate Conversion in Bubble Column Bioreactors

Naresh Kandlapalli

Metabolic Modeling of Bacterial Co-cultures for CO-to-Butyrate Conversion in Bubble Column Bioreactors

A Thesis Presented

by

NARESH KANDLAPALLI

Submitted to the Graduate School of the University of Massachusetts Amherst in partial fulfillment of the requirements for the degree of

MASTER OF SCIENCE IN CHEMICAL ENGINEERING

September 2021

Department of Chemical Engineering

Metabolic Modeling of Bacterial Co-cultures for CO-to-Butyrate Conversion in Bubble Column Bioreactors

A Thesis Presented

by

NARESH KANDLAPALLI

Approved as to style and content by:

_____

Michael Henson, Chair

_____

Jungwoo Lee, Member

_____

Michael Henson, Department Head

Department of Chemical Engineering

ACKNOWLEDGMENTS

First of all, I would like to thank my supervisor, Prof. Michael Henson, for designing this project in the field of renewables. I thank him for the guidance and support which made it my accomplishment to complete this project. I would also like to extend my gratitude to the member of the committee, Prof. Jungwoo Lee, for serving on my thesis committee and for the timely suggestions which he pointed out in this thesis.

I also thank the graduate program director, Prof. Shelly Peyton, for the smooth conduct of the academic program completion. I would also like to thank my group members and friends, especially our alumni, Dr. Xiangan Li, for his constant support and fruitful discussions on this work. It wouldn't have been possible without our alumni, Dr. Poonam Phalak, for her suggestions and support when I first entered the research group.

I would also like to thank my parents for giving me this opportunity to pursue this program with their kind support over the entire course of my graduate studies.

ABSTRACT

Metabolic Modeling of Bacterial Co-cultures for CO-to-Butyrate Conversion in Bubble Column Bioreactors

SEPTEMBER 2021

NARESH KANDLAPALLI

B.E., UNIVERSITY OF MUMBAI

M.S.CH.E., UNIVERSITY OF MASSACHUSETTS AMHERST

Directed by: Professor Michael A. Henson

One of the most promising routes to renewable liquid fuels and chemicals is the fermentation of waste carbon by specialized microbes. Commercial development of gas fermentation technology is underway but many fundamental research problems must be addressed to further advance the technology towards economic competitiveness. This thesis addresses the important problem of developing integrated metabolic and transport models that predict gas fermentation performance in industrially relevant bubble column reactors. The computational models describe the conversion of CO-rich waste streams including synthesis gas to the platform chemical butyrate. The proposed modeling approach involves combining genome-scale reconstructions of bacterial species metabolism with transport equations that govern the relevant multiphase convective and diffusional processes within the spatially-varying system. I compared the combination of the acetogen *Clostridium autoethanogenum* for CO conversion to the intermediate acetate and three different gut bacteria (*Clostridium hylemonae*, *Eubacterium rectale* and *Roseburia hominis*) for conversion of acetate to butyrate. Trial-and-error optimization of

the three co-culture designs was performed to assess their relative performance and guide future experimental studies.

TABLE OF CONTENTS

Page

LIST OF TABLES

Table **Page**

LIST OF FIGURES

Figure **Page**

CHAPTER 1

INTRODUCTION

With global crude oil reserves dropping and demand rising, particularly from developing countries, the pressure on the supply of oil will increase. While the financial crisis of 2007-2010 brought the price of crude oil (per barrel) down from a record high of US$145 in July 2008, factors such as the recovery of global economies and political turmoil in the Middle East have brought the price of crude oil back to US$100. Global reserves of petroleum are expected to be depleted within 50 years at the current rate of consumption [1, 2]. This is desperately needed, combined with the deleterious environmental impacts resulting from the accumulation of atmospheric CO_2 from the combustion of fossil fuels, to produce affordable and environmentally friendly fuels. By legislating mandates and implementing policies to promote research and development (R&D) and commercialization of technologies that allow low-cost low-fossil-carbon fuels to be developed, many countries have responded to this challenge. The European Union (EU) has, for example, required a target for member countries to extract 10% of all transport fuel from renewable sources by 2020 [3]. Renewable energy sources such as solar, wind, and biofuels have been increasing at an annual average rate of 15-50% between 2005 and 2010 [4]. In 2009, renewable energy accounted for an estimated 16% of global consumption of final energy [4]. Biofuels are classified as solid fuels, liquid fuels (biobutanol, bioethanol, and biodiesel), and possible feedstock gaseous fuel like biosyngas (combination of CO, CO_2, and H_2) are derived mainly from biomass [5]. Liquid biofuels made a limited but increasing contribution to the worldwide use of fuels, accounting in 2010 for 2.7% of global road transport fuels [4]. The replacement of fossil fuels to biofuels is necessary to

limit the carbon dioxide gas which is the greenhouse gas that contributes towards the climate change.

Biofuels are made from biomass, which includes seeds, grains, vegetable oils, and animal-based oils, and is derived from a living or recently living organism. Feedstocks are a term used to describe these types of materials. Biomass is organic, which means it is made up of material derived from living organisms like plants and animals. Plants, wood, and waste are the most popular biomass materials used for energy, they are called as biomass feedstocks. Biomass energy can be a non-renewable source of energy. First-generation biofuels are produced from biomass such as sugars and starches, which are widely used as a source of food for humans and animals. Nonfood materials are used to make second-generation biofuels, also known as cellulosic biofuels. Biofuels made from cellulosic materials are not yet commonly available. Ethanol and biodiesel are the two most popular liquid transportation biofuels.

Cellulosic biofuels have the ability to be more environmentally sustainable than first-generation biofuels. Scientists from the Argonne National Laboratory's Center for Transportation Research, the Department of Energy, and Purdue University compared GHG emissions from cellulosic and corn ethanol production in a 2009 report. According to the report, cellulosic ethanol production reduced GHG emissions by 77 percent to 107 percent when compared to gasoline, while corn ethanol production reduced emissions by 24 percent when compared to gasoline [57]. While cellulosic biofuels which provide a solution to many of the criticisms leveled at first-generation biofuels, further research and development is needed before they can be widely distributed. As compared to the cost of

producing conventional gasoline or many first-generation biofuels, the production of cellulosic biofuels is still prohibitively costly.

The alternative technique to the cellulosic technique is the gas fermentation. Syngas fermentation is a microbial process also known as synthesis gas fermentation. Syngas, a mixture of hydrogen, carbon monoxide, and carbon dioxide, is used as a carbon and energy source in this process, and microorganisms turn it into fuel and chemicals [62]. Ethanol, butanol, acetic acid, and butyric acid are the primary components of syngas fermentation [63]. Petroleum mining, steel milling, and methods for processing carbon black, coke, ammonia, and methanol all emit large quantities of waste gases, mostly CO and H_2, into the atmosphere, either directly or by combustion [64]. These waste gases can be converted to chemicals and fuels using biocatalysts and syngas may be used to manufacture fuels and chemicals by a variety of microorganisms.

In this work we focused mainly on the conversion of CO gas to butyrate by experimenting the combinations of acetogen *Clostridium autoethanogenum*, and the gut bacteria *Clostridium hylemonae*, *Eubacterium rectale*, and *Roseburia hominis*, by modeling and simulating a bubble column bioreactor. In bubble column reactors, high mass transfer coefficients can be achieved by using syngas microsparging and/or internal packing to increase gas–liquid interaction. With the CO and H_2 transitions, improved gas–liquid mass transfer also improved syngas consumption. To produce biofuels on a larger scale, bubble column reactors are favorable than the continuous stirred-tank reactors. The whole idea is to use bacteria as bio-catalyst to ferment waste gas like CO into valuable products like ethanol, butyrate, etc. It will be worthwhile to investigate if we could produce some butyrate with gas fermentation.

CHAPTER 2

LITERATURE REVIEW

The fermentation of waste carbon by advanced microbes is one of the most promising routes towards sustainable liquid fuels and chemicals. This would not only allow advanced biofuels and the production of renewable chemicals, but it could also help reduce carbon emissions. This can be achieved by the fermentation of carbon-rich gas to synthesize the desired products like ethanol and 2,3-butanediol [6,8]. Gasification is a mechanism in which feedstock is thermochemically transformed by the use of an agent such as oxygen, steam, air, or supercritical water to carbon monoxide and hydrogen-rich synthesis gas [9-11]. With an overall rate of energy conversion of about 75%–80% [9], this process is successful [9], however CO-rich waste streams are available directly from certain industries and do not require gasification. Gasification has been in use for centuries, although it was the oil crisis of the 1970s that increased interest in the process for heat and power applications and for the development of liquid fuels using Fischer-Tropsch catalysis [10]. Today, coal and petroleum-based technology is the most mature gasification technology in commercial use however, the use of biomass as a feedstock is being intensively researched and developed, as reflected by increased publication and patent activity over the past ten years. Biomass gasification was able to expand on previously developed gasification technology [12], although new technologies were necessary for differences in feedstock and the appropriate composition of synthesis gas for downstream use. Carbon monoxide (CO), hydrogen (H_2), and carbon dioxide ($CO_{2)}$ are the main components of syngas. Other gases, solids, and condensable volatiles [13] will also be contained in syngas derived from biomass. In addition to CO, CO_2, and H_2, water (H_2O);

methane (CH_4); ethene (C_2H_4); ethane (C_2H_6); ethylene (C_2H_2); benzene (C_6H_6); naphthalene ($C_{10}H_8$); ammonia (NH_3) and hydrogen cyanide (HCN); nitrogen oxides (NO_X); sulphur dioxide (SO_2); and hydrogen sulphide (H_2S) and carbonyl sulphide (COS) [13] are the species in the descending order with the highest reported concentrations. Concentrations of these species depend on the constitution of the feedstock and the technique of gasification used [13].

The anaerobic acetogen *Clostridium ljungdahlii*, which develops acetate and ethanol as its primary metabolic by-products [14-16], is the most widely studied gas fermenting bacterium. This has been shown to efficiently transform carbon-rich gas streams via the reconstructed Wood-Ljungdahl pathway [61] into products such as acetate and ethanol [17-18]. As in contrast with *C. ljungdahlii*, a significant benefit of *Clostridium autoethanogenum* is the higher selectivity of ethanol-acetate that can be accomplished without providing H_2, enabling the use of a broader variety of industrial waste gases as feedstock. Wild-type strains of *C. autoethanogenum* and *C. ljungdahlii*, compared with acetate, usually produces low ethanol yields [19-20]. *C. autoethanogenum*, developed by LanzaTech researchers using an iterative selection technique, offers substantially increased selectivity of CO uptake, ethanol-acetate, and ethanol tolerance. [22-23]. Effective mass transfer of gaseous substrates to the culture medium (liquid phase) and microbial catalysts are needed for an optimum gas fermentation system (solid phase). Because of the low aqueous solubility of CO and H_2 at only 77% and 68% of that of oxygen (on a molar basis) at 35 ^{o}C [48], gas-to-liquid mass transfer has been established as the rate-limiting stage and bottleneck for gas fermentation. Therefore, a bioreactor design that delivers adequate

energy-efficient gas-to-liquid mass transfer for gas fermentation on a commercial scale is an important engineering challenge [48].

Gas substrates are continuously fed into the reactor in the continuous stirred tank reactor (CSTR) and mechanically sheared by puzzled impellers into smaller bubbles with a greater interfacial surface area for mass transfer [49]. Furthermore, finer bubbles have a slower increasing velocity and a longer aqueous medium retention time, resulting in a higher transition of gas-to-liquid mass [50]. Microbubble sparger is used in an updated version of CSTR to produce finer bubbles to achieve a higher coefficient of mass transfer [51]. While CSTR provides the microbes with complete mixing and uniform distribution of gas substrates, the high power per unit volume needed to drive the stirrer is thought to make this approach economically unviable for gas fermentation systems on a commercial scale [51]. Gas mixing in the bubble column reactor is accomplished by gas sparging, without mechanical agitation, in comparison to CSTR. This design of the reactor has less moving components and thus has lower capital and operating costs associated with strong heat and mass transfer efficiencies, making it a good choice for large-scale gas fermentation [52].

To experiment the gas fermentation in a bubble column reactor it was studied with in presence of the hydrodynamics to monitor the variables associated to the hydrodynamics like superficial gas velocity, bubble diameter, bubble rising velocity, gas hold up and pressure of gas at each location in a column. In a paper [33], the Henson group investigated the impact of hydrodynamics on bubble column reactor efficiency, by developing spatiotemporal metabolic models for the conversion of CO to ethanol using the microbial catalyst *C. autoethanogenum*. In this paper, they showed how hydrodynamics can be

integrated into the context of reactor modeling and evaluate the effect of hydrodynamics with and without liquid recycling on the efficiency of bubble column reactors. Four different models were created in order to characterize the combined effects of hydrodynamics and liquid recycling. As a function of time and column position, the two models that included hydrodynamics allowed the prediction of superficial gas velocity, gas holdup, gas bubble diameter, and interfacial area. On the assumption that the gas phase was the ideal plug flow plus axial dispersion, the other two models were derived, allowing the hydrodynamic variables to be viewed as constants. In terms of CO conversion, biomass production, and ethanol production, the integration of hydrodynamics has been predicted to significantly decrease bubble column efficiency. Therefore, we concluded that for these complex multiphase processes to generate high fidelity models, the inclusion of hydrodynamics is essential. Our models also predicted that by significantly increasing CO conversion, biomass production, and ethanol and 2,3-butanediol production, liquid recycling increased reactor efficiency compared to a conventional non-recycling configuration [33].

In the co-culture systems [34], an in silico analysis of several systems for the conversion of CO-rich waste gases into chemical butyrate in anaerobic continuous stirred tank bioreactors (CSTBRs) was carried out. Despite having vinyl acetate as a secondary carbon source, *C. autoethanogenum* for CO-to-acetate conversion with the environmental bacterium *Clostridium kluyveri* for acetate-to-butyrate conversion was predicted to yield relatively poor output unless hexanoate production by *C. kluyveri* was removed by in silico metabolic engineering. An alternative design for co-culture focused on the combination of *C. autoethanogenum*, and the curated gut bacterium *Eubacterium rectale* [34]. Because of

the high growth rates and acetate-to-butyrate conversion efficiency with glucose as a secondary carbon source were predicted to provide superior performance without the need for strain engineering. With this wild-type coculture design, the feasibility of large-scale butyrate development was demonstrated via implementation in a simulated bubble column reactor, which predicted improved CO-to-butyrate conversion efficiency for CO-rich feeds containing sufficiently high H_2 levels. With incomplete CO use by *C. autoethanogenum* and CO inhibition of *E. rectale*, co-culture efficiency was predicted to be reduced. The feasibility of bubble column operation was demonstrated for only one co-culture system but was not studied in depth. It indicated that it was possible to further optimize the design of the bubble column and operating parameters. The other type of strain is the engineered *C. autoethanogenum* in which the acetogen is engineered to convert CO to butyrate directly, they worked on this model for the CSTBR with the monoculture [34], it yielded worst performance at higher dilution rate due to limited biomass formation, and for different combination of dilution rate it generated low acetate concentration due to low secretion rates of the engineered strain. The co-culture allowed higher dilution rates to be used, with an expected higher washout value. The optimum value of dilution rate provided better butyrate efficiency which was significantly higher than that achieved in engineered monoculture *C. autoethanogenum*.

In this work, we are considering our previous bubble column model instead of CSTBRs [33], and simulating the bubble column bioreactors for CO-to-butyrate conversion with co-culture combinations of the acetogen *C. autoethanogenum* and the gut bacteria *C. hylemonae*, *E. rectale*, and *R. hominis*. These gut bacteria were selected, based on the performance and versatility in our previous work in the Henson lab (X Li, M Henson,

paper submitted to the Journal of Applied Microbiology). We followed our previous model assuming a homogeneous liquid product or well mixed with recycle and in presence of hydrodynamics [33], but we worked with different microbes. The acetogen secretes acetate as a byproduct which is an intermediate, and the gut microbe uptakes the acetate and it converts it to butyrate. For the growth of these bacteria, it requires the carbon source like for sugar we investigated it using glucose and some essential amino acids and nutrients. In the latter case, we compared the results of each bacterium with the acetogen to check the effect of gas and liquid feed conditions and we also studied the effect of reactor column operating conditions to understand the performance of the column.

CHAPTER 3

MATERIALS AND METHODS

3.1: Genome-scale Metabolic Reconstructions and Flux Balance Analysis

A genome-scale reconstruction (GEM) of the acetogen *C. autoethanogenum* and the three gut bacteria *C. hylemonae*, *E. rectale* and *R. hominis* were followed in this work. We used the wild-type strain of *C. autoethanogenum*, which we used in our previous work [33], and for the gut microbes *C. hylemonae, E. rectale*, and *R. hominis*, we took these strains from an online platform of Virtual Metabolic Human [54]. A broad range of computational methods based on metabolic models have been developed and applied to bacteria, providing useful insights into bacterial metabolism and evolution as well as a solid foundation for computer-aided design in metabolic engineering. We have experimented or have performed the flux balance analysis to check the behavior of each culture. For example, what kind of media can it grow on? What chemical nutrients does it need in what proportions for growth? What is the cell's efficiency in transforming chemicals from the

environment into its own components? What metabolites does it provide or produce with a given set of conditions and essential nutrients? The mass balance constraint can be expressed mathematically for each metabolite that can be "balanced" by a linear equation relating reaction rates of the form $\Sigma S_j V_j = 0$, where S_j is the metabolite's stoichiometric coefficient in reaction j, and V_j is the reaction rate. Reactions that are proven to be thermodynamically irreversible in vivo are constrained to have a non-negative reaction rate in addition to mass balance constraints. Upper limits on reaction rates can also be determined by measurements or theory and incorporated into the model as additional constraints on reaction fluxes [58].

In constraint-based models, reaction rates are described by single numbers called reaction fluxes, which are normalized by the weight of the cells harboring the reactions to account for colony size (a reaction flux is usually expressed with the unit mmol/g dry weight/h). Since the aim is to explain how many metabolic reactions work together, a flux distribution can be thought of as a series of reaction fluxes that covers the entire system. A flux distribution carries enough information to fully characterize a state of the system under the steady-state approximation, which assumes that the concentrations of balanced metabolites are constant. A simple matrix equation can then be used to apply the mass balance constraints on all reaction fluxes using the stoichiometric matrix: $S.V = 0$, where S is the stoichiometric matrix and V is the flux distribution expressed as a vector. The cell considers a flux distribution that is consistent with all of the constraints in a given setting to be achievable (or feasible), whereas one that violates at least one of these constraints is not. One of the framework's key strengths is the simplicity of the system of linear equations that describe constraints, which allows for easy assessments of the viability of a flux

distribution using a computer and standard algorithms. The system is underdetermined and a maximum growth objective is used to form a linear program.

To know this behavior, we performed the flux balance analysis (FBA), as the acetogen *C. autoethanogenum*, requires the gas stream as an input or uptake and it secretes the product acetate, ethanol, and some other by-products. Now for the gut bacteria *C. hylemonae*, *E. rectale*, and *R. hominis*, we treated it with the essential nutrient requirements and carbon sources for their growth, with this we accomplished the results for of the FBA. All the amino acids are divided on considering the carbon C6 basis so because of this if we divide the base value of total amino acids 60 mmol/L parameter to the total number of amino acids for a bacteria and if we multiply it by the carbon number for a particular amino acid that is the initial case for the column. Consider cysteine as a case for the *E. rectale*, so the total amino acid parameter 60mmol/L divides by 4 because *E. rectale* requires 4 amino acids, and then we multiply it by 6/3, because we are considering the C6 basis for each amino acid and the cysteine has 3 carbon number in the formula so the cysteine starts from the calculated value of 30 mmol/L as an initial case.

3.2: Spatial Temporal Metabolic Model of a Bubble Column Bioreactor

Dissolved CO uptake kinetics of *C. autoethanogenum* were specified to follow a modified Michaelis-Menten equation that accounted for CO inhibition, which experimental studies have shown is important at high dissolved CO levels [45],

$$V_{CO} = -\frac{V_{max,CO}\ C_{L,CO}}{K_{m,CO} + C_{L,CO} + \frac{C_{L,CO}2}{K_I}}$$

where V_{co} is the CO uptake rate (mmol/gDW/h), which serves as a bound in the FBA calculation; $V_{max,CO}$ is the maximum CO uptake rate (mmol/gDW/h); $C_{L,CO}$ is the dissolved CO concentration (mmol/L); $K_{m,CO}$ is the CO saturation constant (mmol/L); and K_I is the CO inhibition constant (mmol/L).

C. autoethanogenum uptake of dissolved H_2 was assumed to follow Michaelis-Menten kinetics as,

$$V_{H_2} = -\frac{V_{max,H_2}\ C_{L,H_2}}{K_{m,H_2} + C_{L,H_2}}$$

where V_{H2} is the H_2 uptake rate bound; V_{max,H_2} is the maximum H_2 uptake rate; C_{L,H_2} is the dissolved H_2 concentration; and K_{m,H_2} is the H_2 saturation constant. These uptakes kinetics were studied on the basis of literature review of our past work [35-36]. *C. autoethanogenum* was thought to have the same uptake kinetics for CO and H_2.

Though for the three gut microbes, uptake kinetics for acetate, ethanol, sugar (glucose), butyrate, and the essential amino acids, were adjusted to obey the Michaelis-Menten equation to account for CO inhibition of development [53,34].

$$V_i = -\frac{V_{max,i}\ C_{L,i}}{K_{m,i} + C_{L,i}}\ (1 - \frac{C_{L,CO}}{[CO]_{max}})$$

where V_i is the uptake rate bound of the i -th metabolite (acetate, ethanol, glucose, butyrate, and amino acids); $V_{max,i}$ is the maximum uptake rate, $C_{L,i}$ is the liquid-phase concentration; $K_{m,i}$ is the saturation constant; and $[CO]_{max}$ is the maximum dissolved CO concentration (mmol/L).

The bubble column is assumed to have countercurrent flows of liquid and gas streams with liquid recycle from the bottom of the column to the top of the column (Fig. 1). Because of the higher gas holdup, the key benefit of the recycling column is the ability to achieve high cell concentrations, resulting in better mass transfer, increased CO utilization, and greater synthesis of desired products. The recycling column is more compatible with industrial practice, while traditional columns with co-current gas and liquid flows have been the subject of previous research work [24-25].

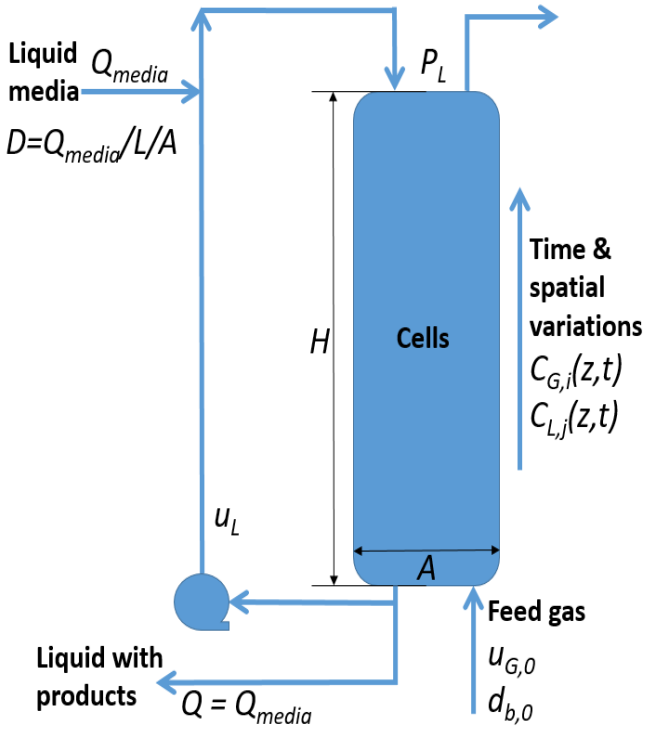

Figure 1: Schematic representation of the countercurrent bubble column reactor model. $U_{G,0}$ and $d_{b,0}$ are the superficial gas velocity and bubble diameter entering the column, U_L is the superficial liquid velocity, H is the reactor height or length, A is the reactor cross-sectional area, P_L is atmospheric pressure, Q_{media} is the media feeding rate, and D is the dilution rate calculated from Q_{media} and the reactor volume.

The co-culture designs were assumed to be well-mixed or homogeneous liquid phase based on previous work [33]. The mass balance equation on the biomass of the i -th species was formulated as,

$$\frac{dX_i}{dt} = \mu_i X_i - DX_i$$

$$X_i\,(0) = X_{i,0}$$

where X_i is the biomass concentration (g/L); μ_i is the specific growth rate (h^{-1}) obtained from solution of the flux balance problem; D is the dilution rate (h^{-1}); and X_0 is the initial biomass concentration.

Mass balance equations on dissolved gas components had the form,

$$\frac{dC_{L,m}}{dt} = v_{1,m}X_1 + v_{2,m}X_2 + k_L a\left(C_m^* - C_{L,m}\right) - DC_{L,m}$$

$$C_{L,m}\,(0) = C_{L,m,0}$$

where $C_{L,m}$ is the dissolved concentration (mmol/L) of m -th gas component (CO and H_2); $v_{i,j}$ is the specific uptake rate of the j -th component by the i -th species; k_{La} is the volumetric gas-liquid mass transfer coefficient, C_m^* is the saturation concentration (mmol/L) of the m –th component calculated from the gas phase concentration using Henry's law at the specified temperature and pressure; and $C_{L,m,0}$ is initial liquid-phase concentration of the m -th component.

Mass balance equations on gas-phase substances had the form,

$$\frac{dC_m}{dt} = \frac{\dot{Q_g}}{V}\left(C_{m,f} - C_m\right) - k_L a(C_m^* - C_{L,m})$$

$$C_m\,(0) = C_{m,f}$$

where C_m is the gas-phase concentration (mmol/L) of the m -th gas component (CO and H_2); $\dot{Q_g}$ is the feed gas volumetric flow rate (L/h); V is the liquid volume (L); and $C_{m,f}$ is the feed concentration (mmol/L) of the m -th gas component.

Mass balances on liquid-phase metabolites had the form,

$$\frac{dC_j}{dt} = v_{1,j}X_1 + v_{2,j}X_2 + D(C_{j,f} - C_j)$$

$$C_j\,(0) = C_{j,f}$$

where C_j is the concentration (mmol/L) of j -th metabolite (glucose, amino acids, butyrate, acetate, and ethanol); $v_{i,j}$ is the specific production (positive) or uptake (negative) rate (mmol/gDW/h) of the j -th metabolite by the i -th species; D is the dilution rate (h^{-1}); and $C_{j,f}$ is the feed concentration of j -th metabolite.

3.3: Hydrodynamics

- The pressure profile was calculated from the liquid head as

$$\frac{dP}{dz} = -\rho_L g \varepsilon_L, \;\; BC: P(H) = P_H$$

where P is the local pressure (Pa), ρ_L is the density of liquid phase (kg·m^{-3}) and assumed to be equal to the density of water, and P_H is atmospheric pressure used as the boundary condition at the top of column.

- The gas holdup was calculated from the one-dimensional drift-flux model,

$$\frac{u_G}{\varepsilon_G} = C_0(u_G + u_L) + v_b(1 - \varepsilon_G)$$

where C_0 is the distribution parameter and v_b is the bubble rising velocity (m·hr^{-1}). The drift-flux model is commonly used for describing the relative motion of multiphase flows without solving the detailed momentum and energy equations [36]. The term v_b (1− ε_G) is related to the weight-average drift velocity [37], and is applicable to the bubbly flow regime and gas holdup less than 25%. The distribution parameter C_0 is often taken as in the range 1 - 1.2 for fast upward bubble flows [38]. A C_0 value of 1.05 was used in this study.

- The equation for bubble rising velocity had the form,

$$v_b = 0.33 g^{0.76} \left(\frac{\rho_L}{\mu_L}\right)^{0.52} \left(\frac{d_b}{2}\right)^{1.28}$$

where g is the gravitational constant (m·s^{-2}), d_b is the bubble diameter (mm), and μ_L is the viscosity of liquid phase (Pa*s). The dependence of the terminal rise velocity of a single bubble on fluid properties has been investigated experimentally by numerous researchers

[38]. Among available correlations, the above equation provides a comprehensive description within its range of applicability [39].

- The equation for bubble diameter had the form [38],

$$d_b = d_{b,0} \sqrt[3]{\frac{P_L n_G}{P n_{G,0}}}$$

where $d_{b,0}$ is the bubble diameter (mm) entering the column, $n_{G,0}$ is the mass flow rate ($g \cdot s^{-1}$) of the feed gas, and n_G is the local molar flow rate ($g \cdot s^{-1}$) of the gas stream. We treated $d_{b,0}$ as an operating variable. In practice, the bubble diameter can be controlled by appropriate design of gas spargers [40]. This relation accounted for increasing bubble size due to decreasing pressure and decreasing size due to gas consumption.

- Using the ideal gas law, the following equation was derived for the superficial gas velocity,

$$u_G = u_{G,0} \frac{P_L}{P} \frac{n_g}{n_{g,0}}$$

where $u_{G,0}$ is the superficial velocity ($m \cdot hr^{-1}$) of the feed gas entering the column.

- The interfacial gas–liquid mass transfer area was calculated as [41-42],

$$a = \frac{6\varepsilon_G}{(1 - \varepsilon_G) d_b}$$

Table 1: Operating parameter values of the bubble column reactor

Parameter	Symbol	Value	Source
Column height or length	H or L	10 m	Specified
Column cross-sectional area	A	3 m^2	Specified
Pressure at the top of column	P_H	1.013e5 Pa	Specified
Temperature	T	37 ℃	Specified
Feed superficial gas velocity at 1 atm	$U_{G,0}$	100 m/h	Specified
Superficial liquid phase velocity	U_L	50 m/h	Specified
Feed gas bubble diameter at 1 atm	$d_{b,0}$	1.5 mm	Specified
Gas-liquid mass transfer coefficient	k_L	1e-4 m/s	[33]
Liquid phase dispersion coefficient	D_L	0.25 m^2/h	[33]
CO mole fraction in feed gas	y_{CO}	70%	Specified
N_2 mole fraction in feed gas	y_{N2}	30%	Specified
Dilution rate	D	0.14 h^{-1}	Specified
CO Henry's law constant	H_{CO}	8e-4 mol/L/atm	[33]
H_2 Henry's law constant	H_{H2}	6.6e-4 mol/L/atm	[25]
Viscosity of liquid phase	μ_L	0.9242 mPa*s	[33]
Distribution parameter for drift-flux model	C_0	1.05	[33]
Initial biomass concentration	X_i	0.01 g/L	Specified
Maximum CO uptake rate	$V_{CO,m}$	50 mmol/gDW/h	[34]
CO saturation constant	$K_{m,CO}$	0.1 mmol/L	[34]
CO inhibition constant	$K_{L,CO}$	5 mmol/L	[34]
Maximum H_2 uptake rate	$V_{H2,m}$	50 mmol/gDW/h	[34]
H_2 saturation constant	$K_{m,H2}$	0.1 mmol/L	[34]
Initial feed glucose concentration	G_i	200 mmol/L	Specified
Total amino acids	Taa	60 mmol/L	Specified
Maximum glucose uptake rate	$V_{G,m}$	10 mmol/gDW/h	[34]
Maximum total amino acids uptake rate	$V_{taa,m}$	1 mmol/gDW/h	Specified
Glucose saturation constant	$K_{m,G}$	0.5 mmol/L	[34]
Maximum dissolved CO inhibition concentration	$[CO]_{max}$	0.7 mmol/L	[33]
Maximum uptake rate for acetate and ethanol	$V_{i,m}$	5 mmol/L	[34]
Saturation constant for acetate and ethanol	$K_{m,i}$	0.5 mmol/L	[34]

The bubble column length L and cross-sectional area A correspond to a typical length-to-diameter ratio of 5 [43], and a reactor volume of 30,000 L consistent with a demonstration-scale unit for a column length of 10 m and column cross-sectional area of 3

m^2. The pressure P_H at the top of the column is atmospheric, and the temperature T is optimal for the acetogen *C. autoethanogenum* and the gut bacteria growth [44].

The feed superficial gas velocity $u_{G,0}$ and bubble diameter $d_{b,0}$ were specified at atmospheric pressure and were pressure corrected as follows to calculate the actual feed conditions:

$$u_{G,f} = u_{G,0}\frac{P_L}{P}, d_b = d_{b,0}\sqrt[3]{\frac{P_L}{P_0}}$$

3.4: Numerical Solution

The models of the bubble column consisted of linear programs (LP) for the cultures intracellular metabolism, algebraic equations (AEs) and ordinary differential equations (ODEs) in two-phase hydrodynamics space, ODEs for liquid-phase mass balances in time, and partial differential equations (PDEs) for gas and dissolved gas mass balances in time and space. Based on spatial discretization of the PDEs, we adopted our previously established numerical solution strategy. In this working model, we simulated it for 21 node points, each separated by 0.5 m, the reactor height was discretized and spatial derivatives and boundary conditions were approximated by central finite differences [25], Using DFBAlab [55-56], a MATLAB code for effective and robust solution of dynamic flux balance models, the resulting differential algebraic equation (DAE) system with embedded LPs was solved. To ensure that LP solutions remained unique despite the possibility of alternative optima, DFBAlab required the concept of hierarchical optimization goals [56].

The MATLAB code involves, ode15s for DAE solution and Gurobi for LP solution were used by DFBAlab. The solution of ODE-LP systems was required by our previous bubble column models (Chen et al., 2015, 2016), while the current models needed the solution of DAE-LP systems because of the introduction of two-phase hydrodynamics. We considered the definition of consistent initial conditions to be difficult for the DAE systems, as we introduced the hydrodynamics for each node points to formulate the initial condition. Inspired by the proposed initialization methods (Vieira & Biscaia, 2001), we developed a robust DAE initialization strategy that avoided the problem of initial conditions that were inconsistent. Second, it integrated a bubble column model without hydrodynamics and captured the steady-state solution. This solution was used to measure the hydrodynamic variables' steady-state values. To produce initial conditions for the bubble column model with hydrodynamics, the steady-state solutions were combined. This method produced "almost" consistent initial conditions that allowed MATLAB to find the parameters of the nominal model to be consistent initial conditions. This initial condition induced convergence when parameter modifications were introduced if the parameter change was sufficiently small. Otherwise, in several smaller steps, the parameter change was implemented to generate a sequence of initial conditions that allowed convergence.

CHAPTER 4

RESULTS & DISCUSSIONS

4.1: Flux Balance Analysis

We performed the flux balance analysis (FBA) of the acetogen *C. autoethanogenum* (Fig. 2), and the gut microbes *C. hylemonae* (Fig. 3), *E. rectale* (Fig. 4), and *R. hominis* (Fig. 5) to get a clear idea of the behavior of these bacteria performance. We worked on feeding the carbon sources glucose and investigated that the essential amino acids differed for each microbe wherein cysteine, glutamate, methionine, and tryptophan were required for the gut microbe *C. hylemonae* to grow in the column, for *E. rectale* essential amino acids were cysteine, glutamate, methionine and leucine, but *R. hominis* required five amino acids and those were cysteine, glutamate, methionine, leucine and alanine.

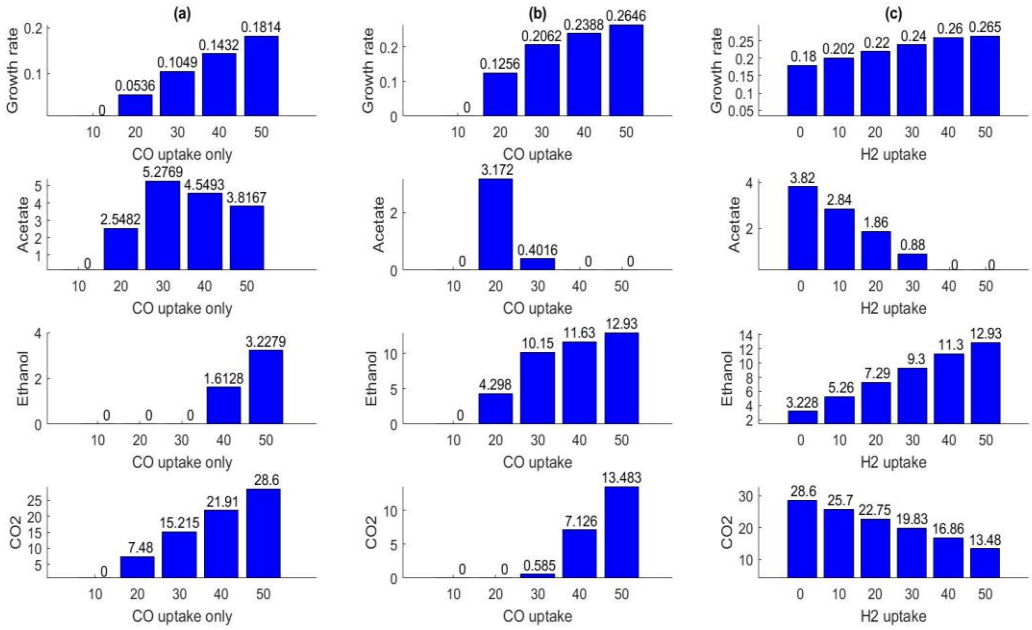

Figure 2: Flux balance analysis of *C. autoethanogenum*. (a) Analysis at varying CO uptake only without considering H_2; (b) analysis at varying CO uptake keeping H_2 at base value of 50 mmol/gDW/h; (c) analysis at varying H_2 uptake with CO at base value of 50 mmol/gDW/h. Growth rate is in h^{-1}, and the rest of other components are in mmol/gDW/h.

The acetogen grows with a maximum growth rate of 0.265 mmol/gDW/h but in the flux profile (Fig. 8), it is seen that the growth is 0.1814 mmol/gDW/h at which the acetate, ethanol and carbon dioxide (CO_2) is secreted by the acetogen. At the base case, when we set the CO and H_2 uptake of 50 mmol/gDW/h we achieve the growth rate of 0.1814 mmol/gDW/h which is evident with the dynamic flux balance analysis (DFBA) simulation results (Fig. 8). Acetate and ethanol production is an important factor since they are crossfed in the co-culture system. Ethanol in column (a) of Figure. 2, represents the analysis when H_2 is not considered, it is clear that if CO is uptaken at low rates then the ethanol is not produced but for higher rates of CO some ethanol is produced, and acetate on the other hand is producing at each rate. If H_2 at base value 50 mmol/gDW/h is considered in the feed or if the system uptakes it in column (b), while changing the CO uptake then ethanol production is dominating with higher rate than the acetate, because the CO converts the most acetate not H_2. Now we also analyzed keeping the CO at base value 50 mmol/gDW/h and changing H_2 uptake rate in column (c). In this case the results looked promising because the acetate is produced for each lower rate of H_2, and the ethanol is minimum at that point.

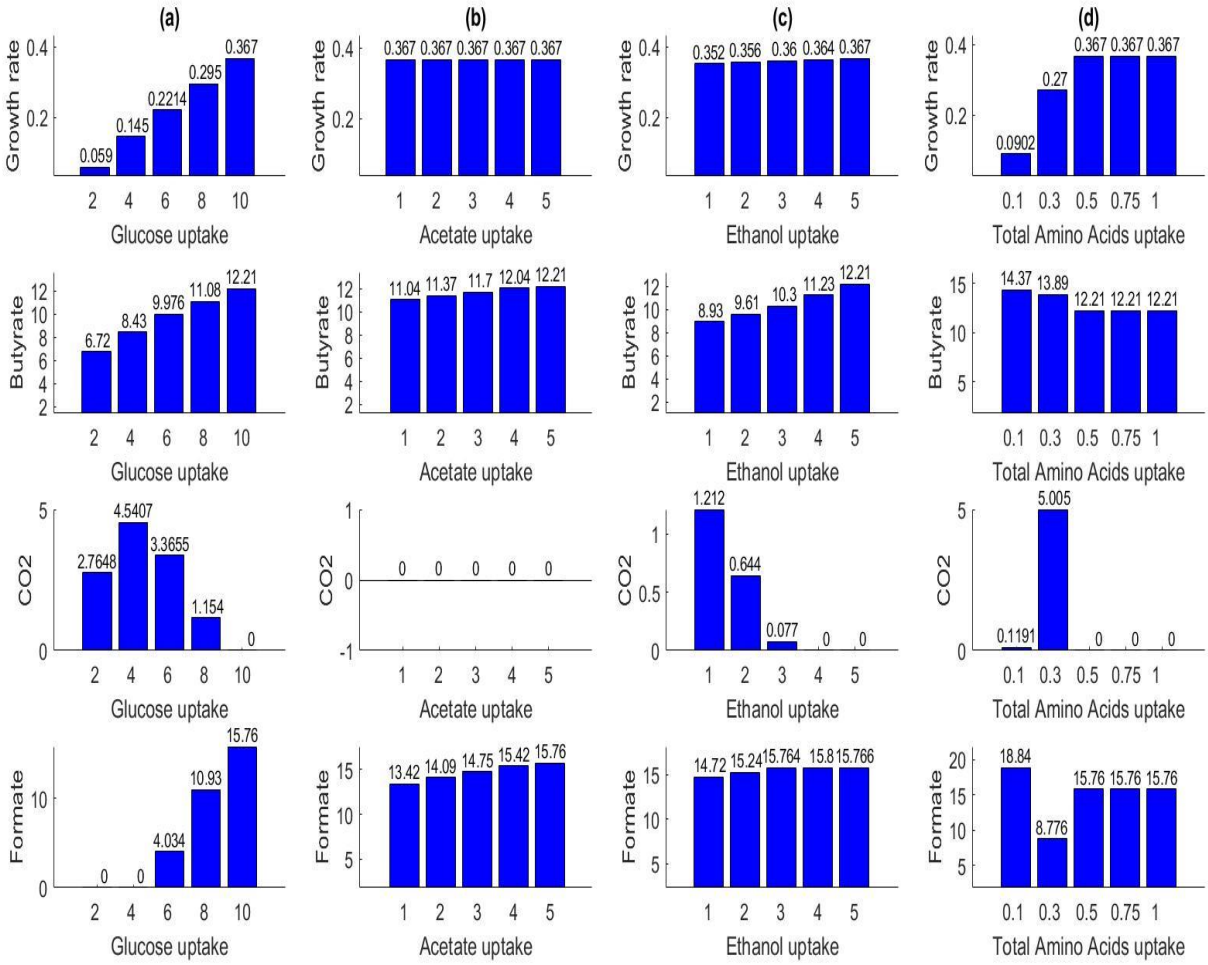

Figure 3: Flux balance analysis of *C. hylemonae*, at varying (a) glucose uptake, (b) acetate uptake, (c) ethanol uptake and (d) total amino acids uptake in mmol/gDW/h; keeping the base value for each parameter at maximum uptake glucose 10 mmol/gDW/h, acetate 5 mmol/gDW/h, ethanol 5 mmol/gDW/h, and total amino acids at 1 mmol/gDW/h.

We also added the essential common ions, and minimum medium requirement for each bacterium to grow. The acetogen uptakes gas CO, H_2 and it secretes the by-products acetate, ethanol and CO_2 in this case, wherein the gut microbe uptakes the acetate and ethanol formed by the acetogen and it converts it to the butyrate product. By performing these flux balance analysis, we also get the results of the by-products at varying uptakes in mmol/gDW/h.

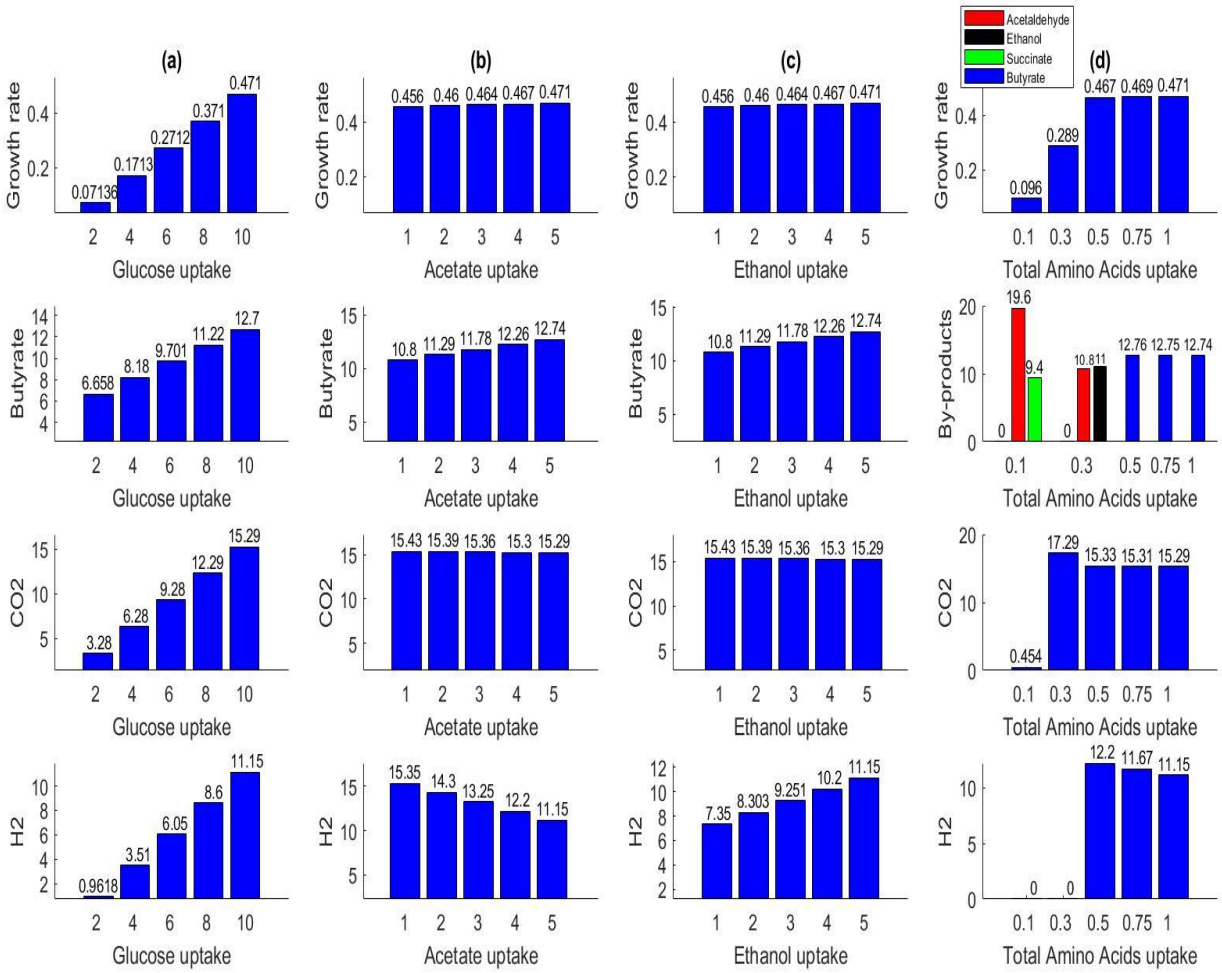

Figure 4: Flux balance analysis of *E. rectale*, at varying (a) glucose uptake, (b) acetate uptake, (c) ethanol uptake and (d) total amino acids uptake in mmol/gDW/h; keeping the base value for each parameter at maximum uptake glucose 10 mmol/gDW/h, acetate 5 mmol/gDW/h, ethanol 5 mmol/gDW/h, and total amino acids at 1 mmol/gDW/h.

Now, we scrutinized the gut microbe's behavior by performing the FBA with varying uptakes by keeping the other value at the base value, the *C. hylemonae* bacteria had the maximum growth rate that can attain at base case with 0.367 mmol/gDW/h, butyrate with the rate of 12.21 mmol/gDW/h, and with the other by-products of CO_2 and formate. In the case of *E. rectale* (Fig. 4), we got an interesting results in which if we uptake the total amino acids as low as 0.1 and 0.3 mmol/gDW/h, then butyrate was affected by this and there were some other by-products like acetaldehyde, ethanol, and succinate. The growth rate for the *E. rectale* stood to be 0.471 mmol/gDW/h which is 22% greater than

the *C. hylemonae* and in this case we also achieved the hydrogen (H_2) by-product which can be crossfed.

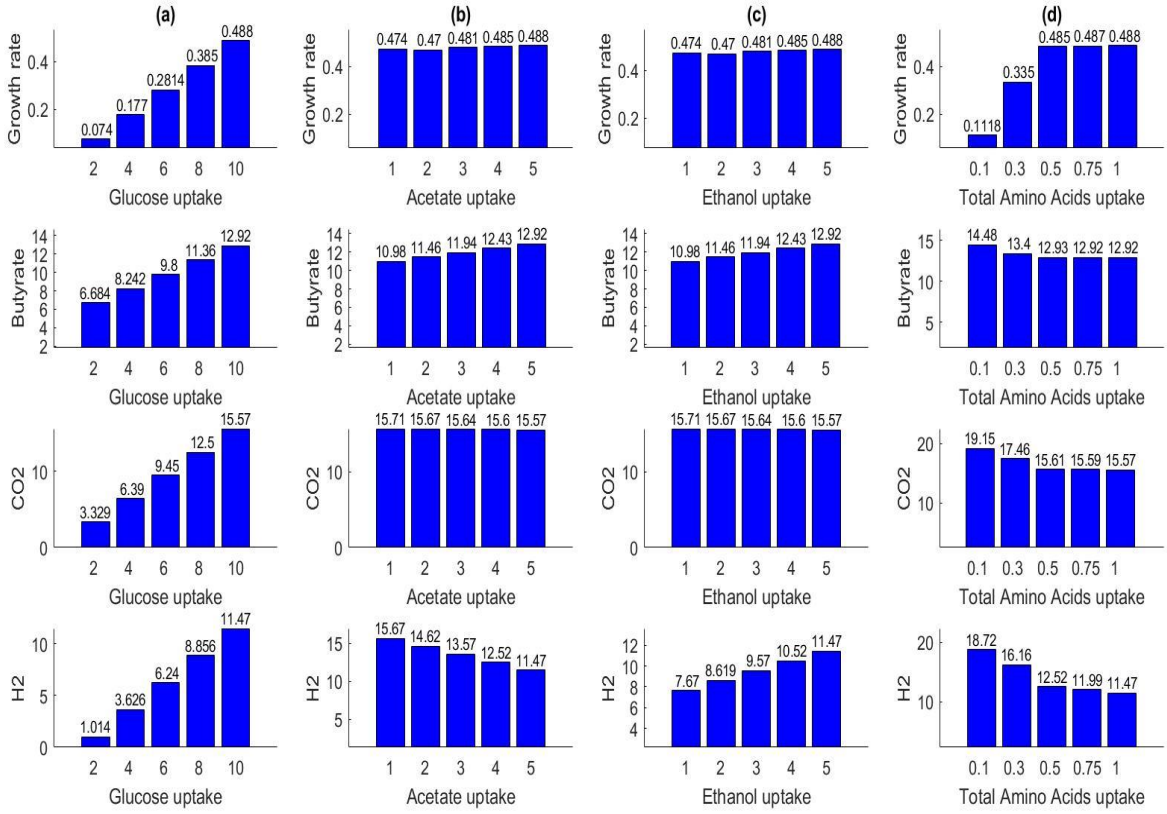

Figure 5: Flux balance analysis of *R. hominis*, at varying (a) glucose uptake, (b) acetate uptake, (c) ethanol uptake and (d) total amino acids uptake in mmol/gDW/h; keeping the base value for each parameter at maximum uptake glucose 10 mmol/gDW/h, acetate 5 mmol/gDW/h, ethanol 5 mmol/gDW/h, and total amino acids at 1 mmol/gDW/h.

The *R. hominis* (Fig. 5), had a similar result compared to the *E. rectale* with the maximum growth rate which it can attain at the base value was 0.488 mmol/gDW/h, but for the hydrogen by-product it seemed to perform better than the *E. rectale* at lower total amino acids uptake rates. Now, we will perform the dynamic flux balance analysis (DFBA) simulation results to understand how it would impact in the bubble column bioreactor spatially at each location of the column.

4.2: Bubble Column Co-culture Simulations

Dynamic flux balance analysis (DFBA) of the column were performed (Fig. 6), for each microbe combination with the acetogen *C. autoethanogenum* at gas feed composition 70/30 (CO/N_2), and due to the large reactor volume of the column our base case carbon source parameter value were 200 mmol/L of glucose, 60 mmol/L of total amino acids. The essential amino acids, cysteine, glutamate, methionine, tryptophan are for the *C. hylemonae*, leucine replaces tryptophan for the *E. rectale*, but the *R. hominis* requires an addition of amino acid which is alanine and the rest of amino acids are same for *E. rectale*. In these simulations I have analyzed the biomass of each bacterium, CO in gas and CO in liquid phase, carbon sources like glucose and all the essential amino acids, and the liquid products exiting the column dynamically for 500 hours to examine of bubble column reactor at 70/30 (CO/N_2) gas feed composition.

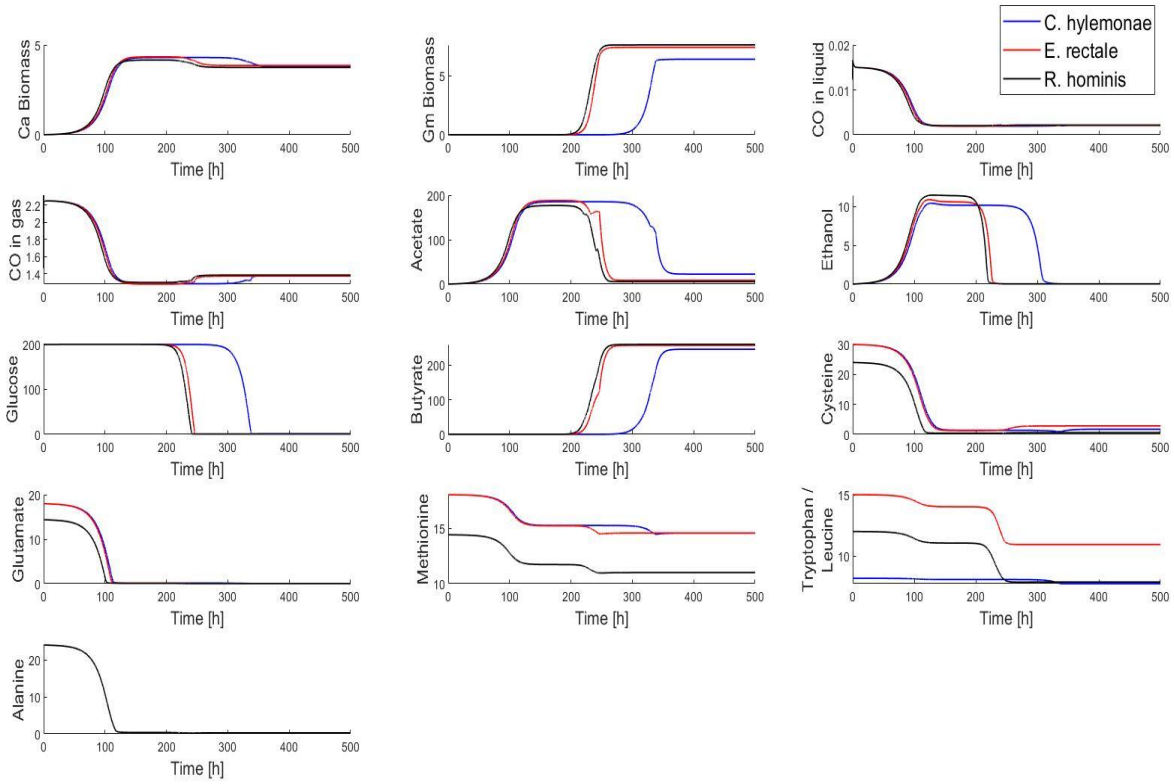

Figure 6: Co-culture dynamic profiles of the liquid stream products exiting the column at the gas feed composition 70/30 (CO/N_2). These conditions are referred to as the base case. Ca is the acetogen *C. autoethanogenum*, Gm are the gut microbes *C. hylemonae*, *E. rectale* & *R. hominis*. Biomass is in g/L, the CO in liquid, CO in gas, acetate, ethanol, glucose, butyrate concentration, and the amino acids cysteine, glutamate, methionine, tryptophan, leucine, alanine are in mmol/L.

It is clear from the above results (Fig. 6) that *C. hylemonae* takes more time to consume glucose and to secrete the product butyrate, unlike *E. rectale* and *R. hominis*, and comparatively the *C. hylemonae* gives less biomass. Then I looked at the spatial steady state profile (Fig. 7), and since I assumed it to be a homogeneous liquid product so the values at each location of the column are steady. In this case the *E. rectale* and *R. hominis* are superior in terms of the butyrate concentration because the *C. hylemonae* gives 5% less concentration of butyrate.

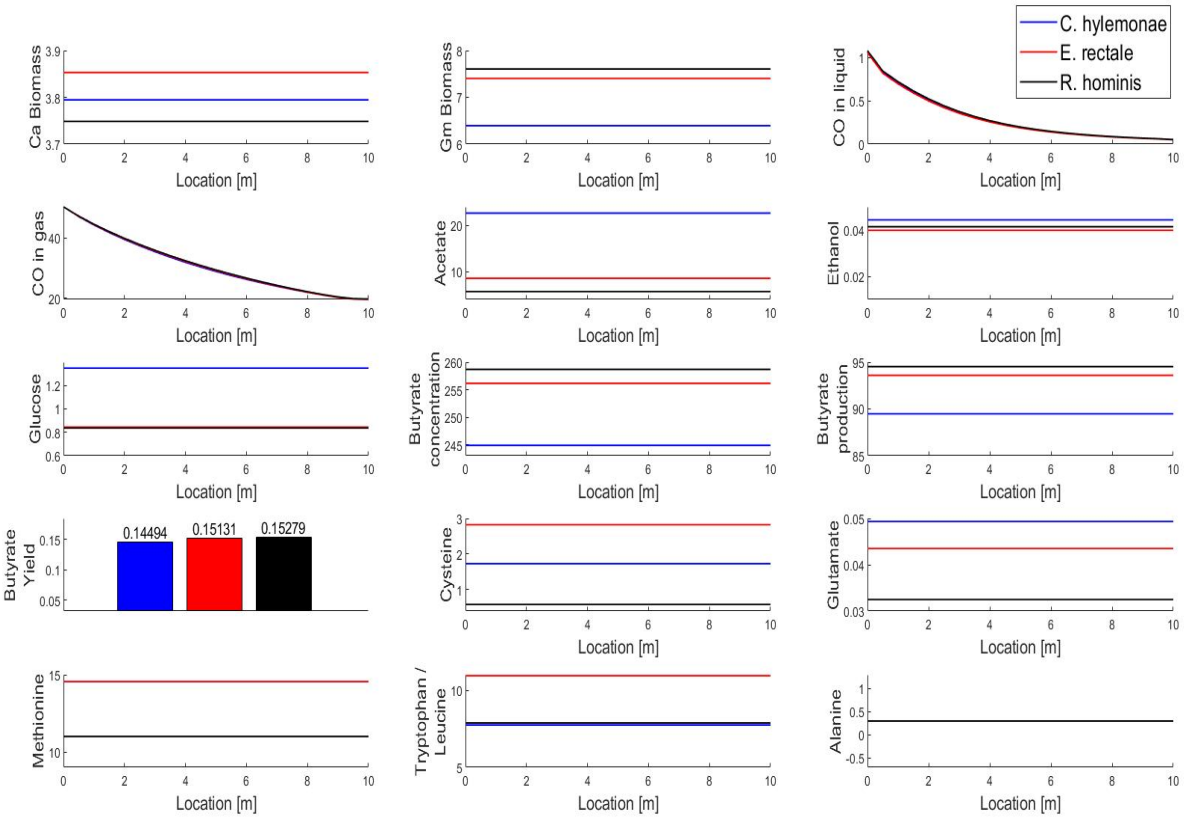

Figure 7: Spatial steady state profile of the liquid stream products exiting the column at the gas feed composition 70/30 (CO/N_2). These conditions are referred to as the base case. Ca is the acetogen *C. autoethanogenum*, Gm are the gut microbes *C. hylemonae*, *E. rectale* & *R. hominis*. Biomass is in g/L, the CO in liquid, CO in gas, acetate, ethanol, glucose, butyrate concentration, and the amino acids cysteine, glutamate, methionine, tryptophan, leucine, alanine are in mmol/L. Butyrate production is in kg/h.

The relationship of the fluxes are shown below (Fig. 8), I performed it dynamically to check the behavior of the growth rate of a microbe, the gas rate and the other carbon sources which are required in a system. This analysis gives an idea of how the fluxes perform at each location in the column. It is noticeable that the acetogen growth rate decreases with increasing column location and the gut bacteria growth rate increases while up taking the glucose at location close to 2m of the column. We can see that the acetogen consumes amino acids methionine and leucine as well; the acetate (intermediate) is

consumed by the microbes which are produced by the acetogen *C. autoethanogenum* at location 5m, and the butyrate synthesis rate begins at location close to 2m of the column.

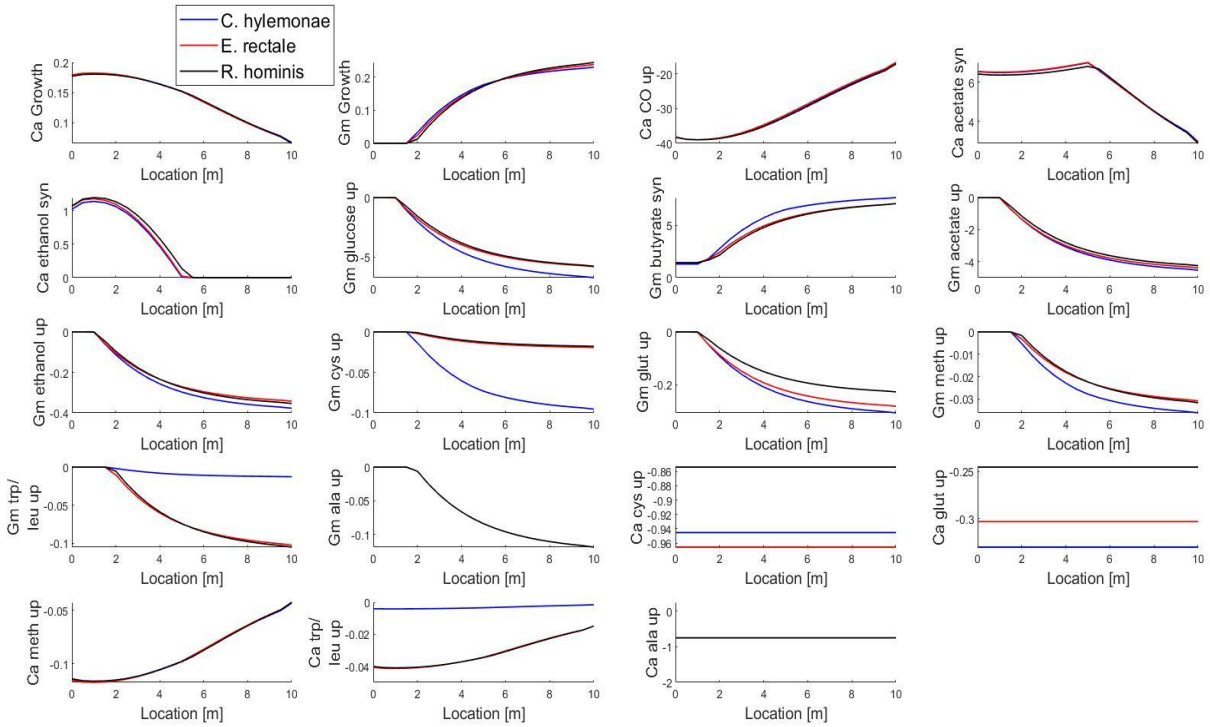

Figure 8: Spatial flux profile at the gas feed composition 70/30 (CO/N_2). These conditions are referred to as the base case. Ca growth is the acetogen *C. autoethanogenum* growth rate in h^{-1}, Gm are the gut microbes *C. hylemonae, E. rectale* & *R. hominis*, growth rate in h^{-1}, and the rest of components are in mmol/gDW/h, +ve values indicate that it is the synthesis rate other than the growth rate, -ve values indicates the uptake rate. The four amino acids, cysteine (cys), glutamate (glut), methionine (meth), tryptophan (trp), leucine (leu), and alanine (ala), spatial fluxes are represented at each location of the column, with the metabolite acetate and ethanol flux for each culture, butyrate synthesis rate of the gut microbe. The performance of the gut microbe glucose uptake rate and the CO uptake of the acetogen is shown at each location in the column.

To examine the process at varying gas feed composition we added hydrogen (H_2) and the results (Fig. 9) are completely different when we change the feed composition or if we add hydrogen. If we compare it with 70/30 CO/N_2 composition the *C. hylemonae* is superior with the butyrate concentration and production with 20% yield, and this is because of the better CO conversion which impacted with less amount of CO gas composition in the feed.

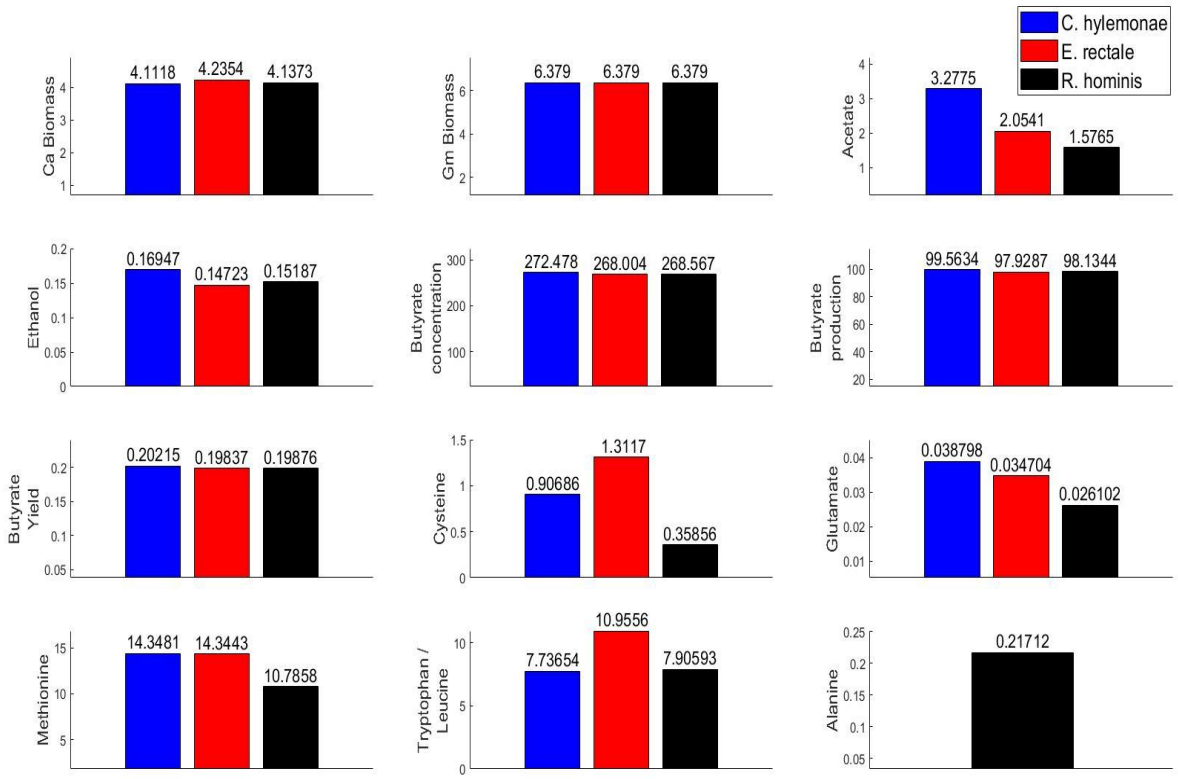

Figure 9: Steady state values of the liquid stream products exiting the column at the gas feed composition 50/30/20 ($CO/N_2/H_2$). These conditions are referred to as the base case. Ca is the acetogen *C. autoethanogenum*, Gm are the gut microbes *C. hylemonae, E. rectale* & *R. hominis*. Biomass is in g/L, the CO in liquid, CO in gas, acetate, ethanol, glucose, butyrate concentration, and the amino acids cysteine, glutamate, methionine, tryptophan, leucine, alanine are in mmol/L. Butyrate production is in kg/h.

4.3: Effect of Gas and Liquid Feed Conditions

Dilution rate is the key parameter dealing with the bioreactor which describes the relationship between the flow of the media into the bioreactor and the culture volume within the bioreactor. It also helps to scale-up the bioreactor to maximize the biochemical production, as it covers the minimum medium requirement in the feed and the carbon sources which is required for the growth of the bacteria in the bioreactor or the column. We further examined the sensitivity analysis to check if the column can perform at varying dilution rate (Fig. 10) with a 10m column length. *C. hylemonae* washed out at 0.16 h^{-1} dilution rate for 70/30 CO/N_2 feed composition but it worked well for 0.16 h^{-1} dilution rate

in addition of hydrogen as a feed (Fig. 11). The unconsumed acetate for *C. hylemonae* was more if we compare with *E. rectale* and *R. hominis* for 70/30 CO/N_2 gas feed, and also it secreted 5% less butyrate concentration, but in addition of hydrogen again as we noticed that *C. hylemonae* performed better in that case so here is the trade-off between two gas feed combinations. With increasing dilution rate, the butyrate concentration decreases but the butyrate production decreases and this is because for the production in kg/hr we consider the area, length of the column and dilution rate.

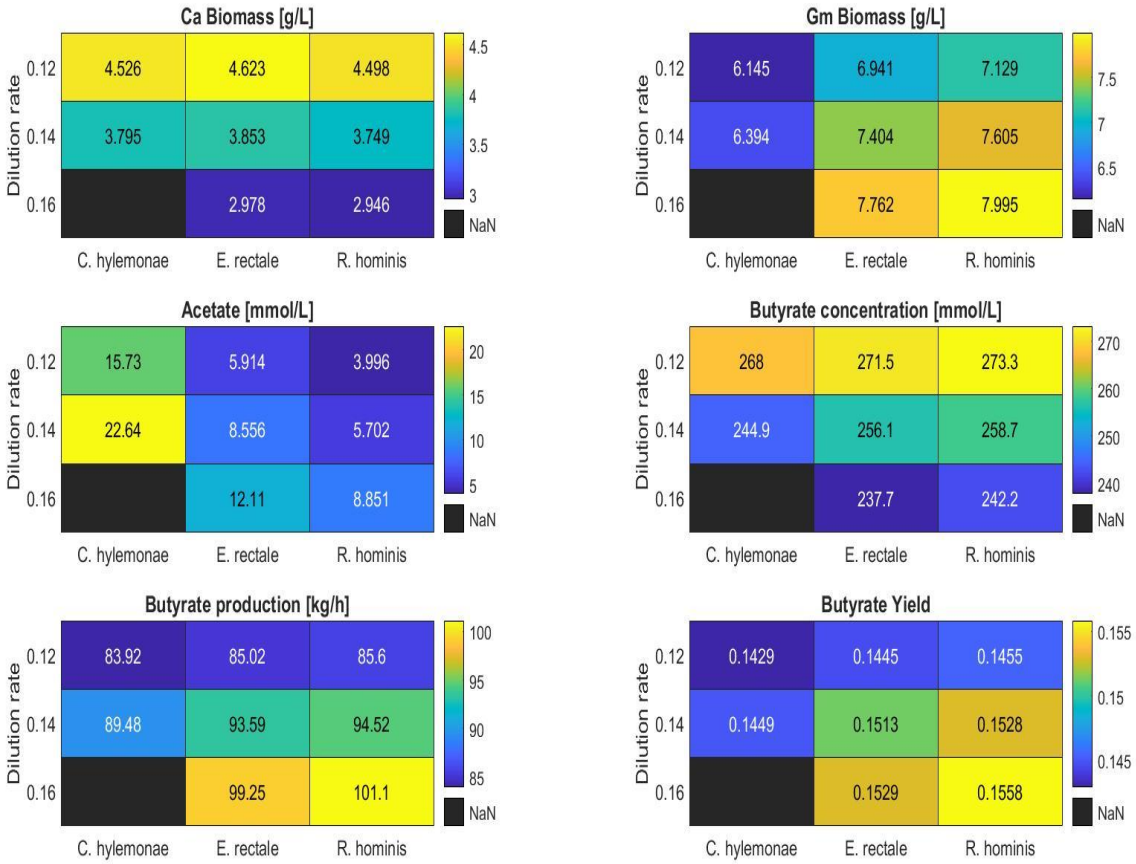

Figure 10: Steady state values of the liquid stream products exiting the column at the gas feed composition 70/30 (CO/N_2), and at varying dilution rates in h^{-1}. Ca is the acetogen *C. autoethanogenum*, Gm are the gut microbes *C. hylemonae*, *E. rectale* & *R. hominis*. NaN is not a number or zero.

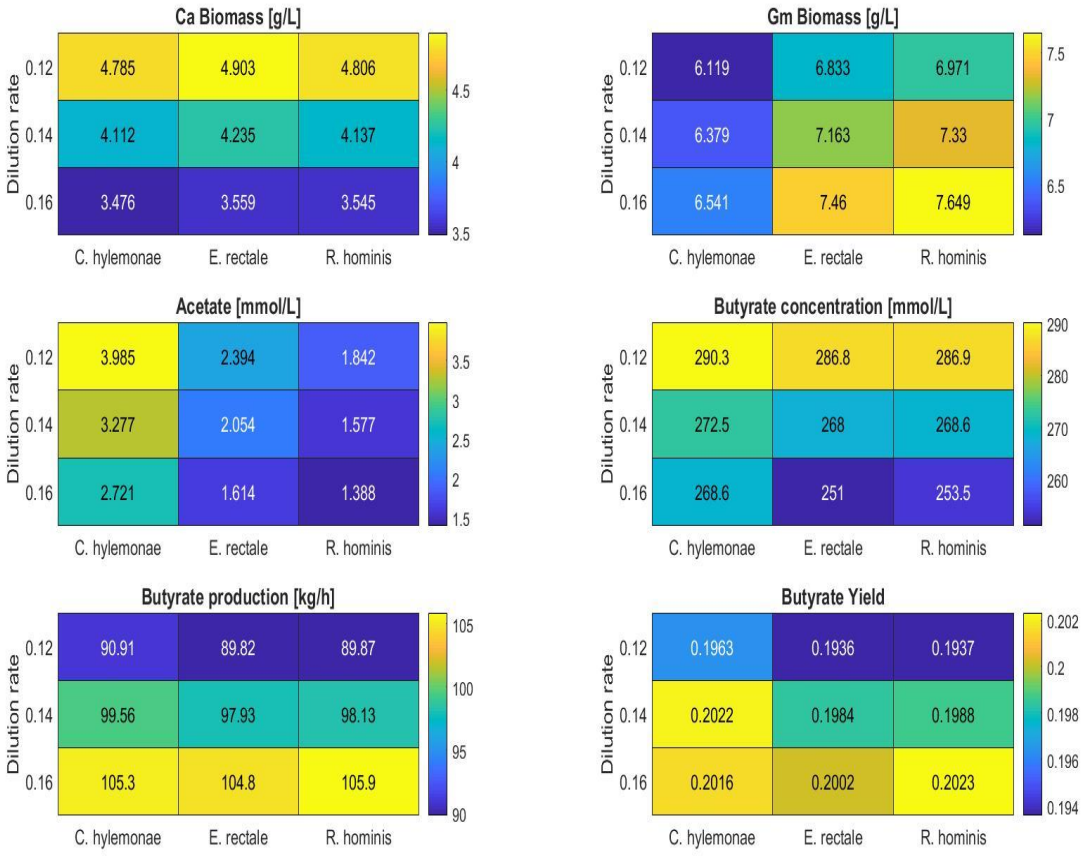

Figure 11: Steady state values of the liquid stream products exiting the column at the gas feed composition 50/30/20 ($CO/N_2/H_2$), and at varying dilution rates in h^{-1}. Ca is the acetogen *C. autoethanogenum*, Gm are the gut microbes *C. hylemonae*, *E. rectale* & *R. hominis*.

Now I studied the carbon sources like glucose and the amino acid requirement, and analyze how it changes if we provide the operating parameter of those at below and above the base case value of 200 mmol/L of glucose and 60 mmol/L of total amino acids. I explored the initial glucose concentration parameter with the range at which the glucose can be consumed from 175 mmol/L to 225 mmol/L with base case value of 200 mmol/L. The below heat-map (Fig. 12), shows the simulation steady state values of the liquid stream products exiting the column at the gas feed composition 70/30 CO/N_2, and the other gas feed composition 50/20/30 $CO/H_2/N_2$ is also shown (Fig. 13) for comparison of results.

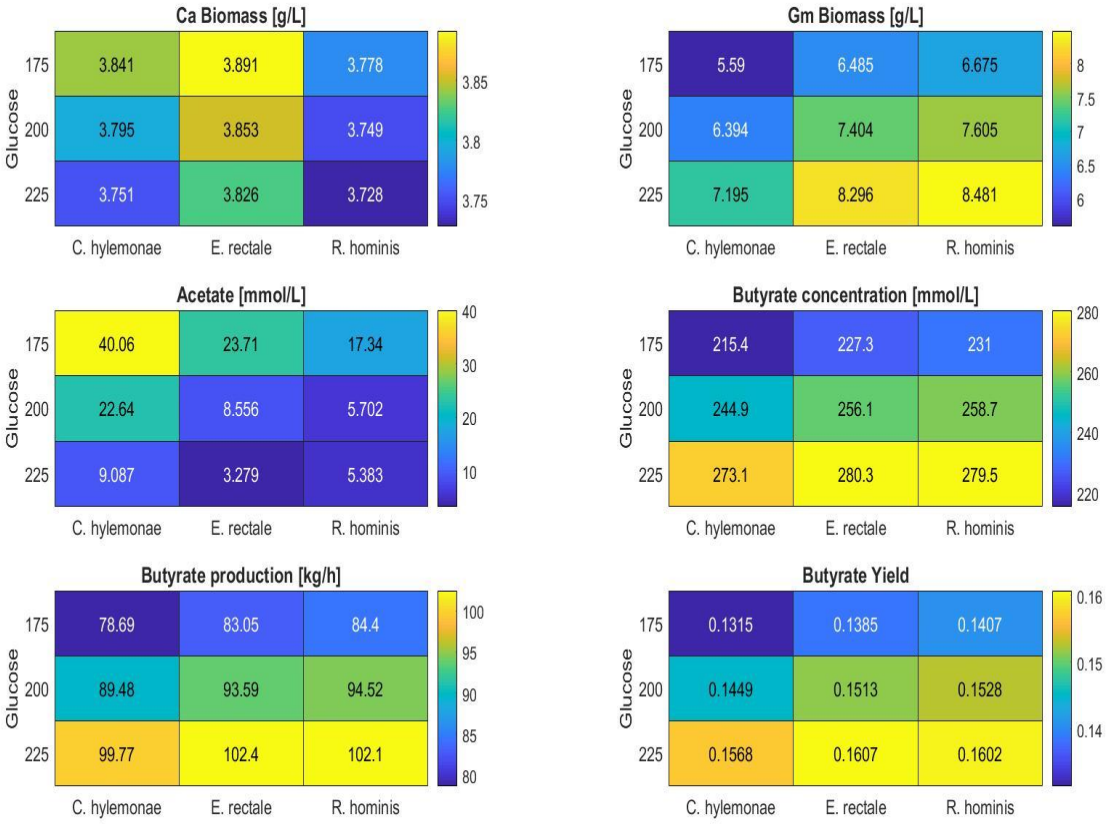

Figure 12: Steady state values of the liquid stream products exiting the column at the gas feed composition 70/30 (CO/N_2), and at varying glucose in mmol/L. Ca is the acetogen *C. autoethanogenum*, Gm are the gut microbes *C. hylemonae*, *E. rectale* & *R. hominis*.

The problem is we can use glucose at higher concentration but the ultimate aim is to optimize as low as it can so that the cost is not impacted. If we compare the 200 mmol/L and 225 mmol/L results for each microbe it shows that the acetate for *C. hylemonae* is not converted much to butyrate which means it demands more glucose to convert it fully which is not our goal. In the case of hydrogen in feed (Fig. 13), *C. hylemonae* tends to convert more acetate to butyrate.

To find a favorable combination to the glucose concentration, I further investigated the study of total amino acid parameter to diversify the results while operating the bubble column reactor keeping the base value of glucose at 200 mmol/L, dilution rate 0.14 h^{-1}, and 10 m column length.

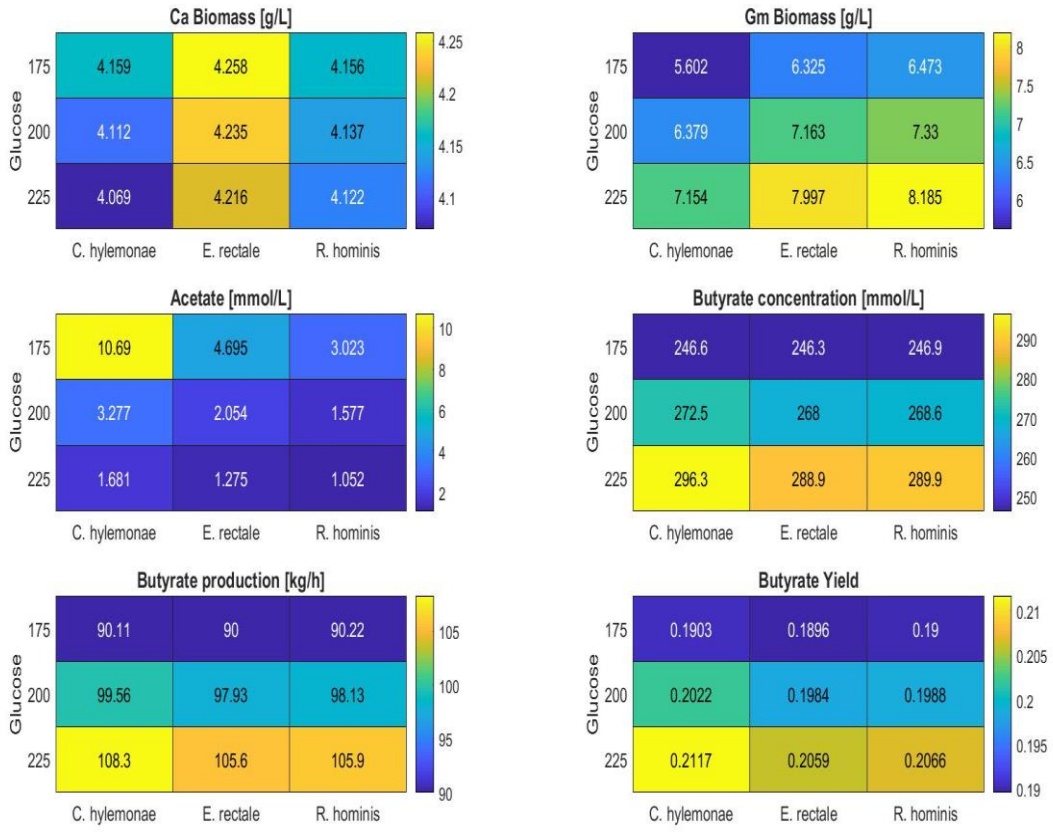

Figure 13: Steady state values of the liquid stream products exiting the column at the gas feed composition 50/30/20 ($CO/N_2/H_2$), and at varying glucose in mmol/L. Ca is the acetogen *C. autoethanogenum*, Gm are the gut microbes *C. hylemonae*, *E. rectale* & *R. hominis*.

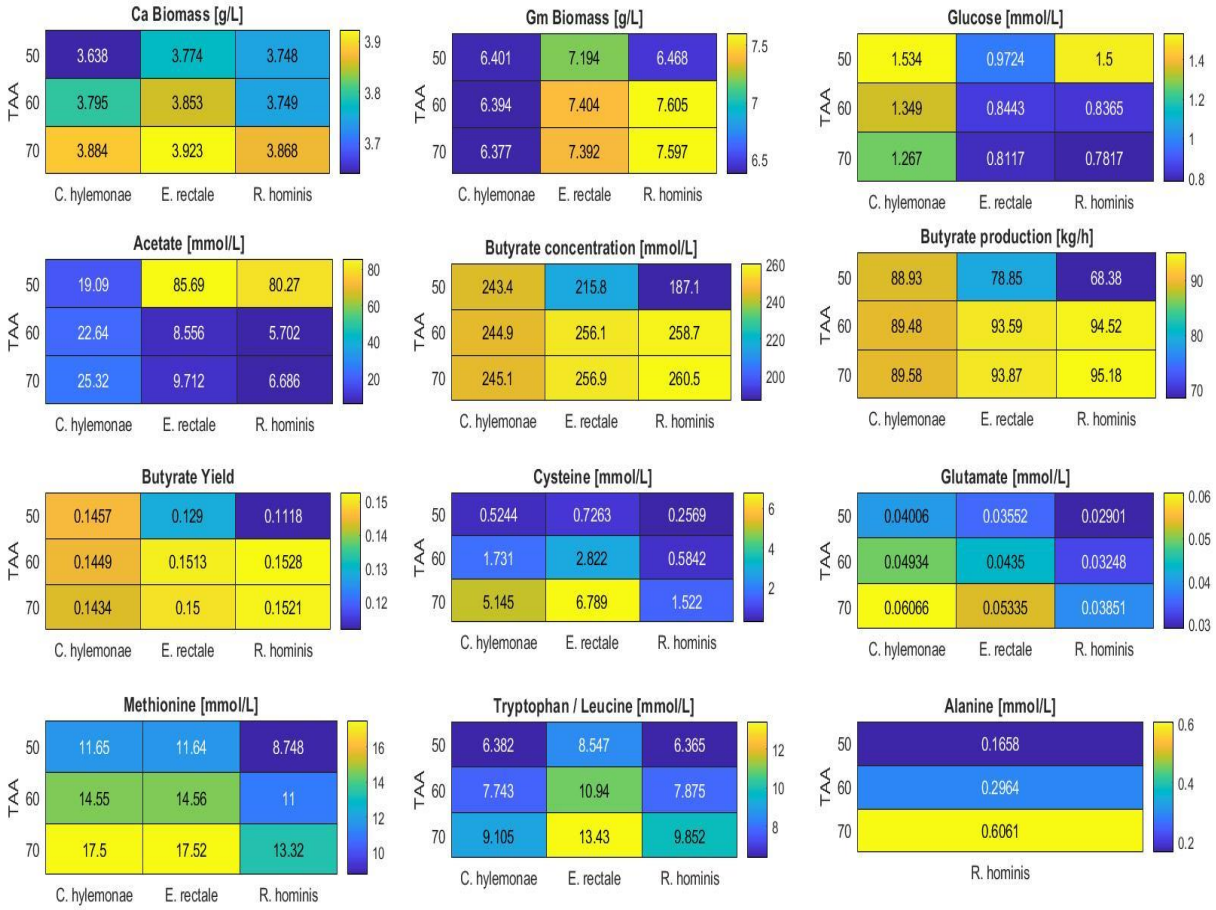

Figure 14: Steady state values of the liquid stream products exiting the column at the gas feed composition 70/30 (CO/N_2), and at varying total amino acids (TAA) in mmol/L. Ca is the acetogen *C. autoethanogenum*, Gm are the gut microbes *C. hylemonae*, *E. rectale* & *R. hominis*.

The above figure represents the liquid product stream exiting the column at gas feed composition 70/30 CO/N_2 and at varying total amino acid parameter. Amino acids are more expensive than glucose, so it is better to treat at low concentrations if we get good amount of butyrate production considering the other aspect of recycling the liquid amino acids coming out of the column. *C. hylemonae* shows some positive results at low concentration (Fig. 14) of 50 mmol/L as most of the acetate is converted, and the butyrate concentration is 243.4 mmol/L which is 11.33 % more than the *E. rectale*, and 23% more than the *R. hominis*, but *C. hylemonae* doesn't change much at higher concentrations of amino acids.

If we compare each amino acid, then it is clear that the cysteine and glutamate is consumed fully by each gut microbe, and for *R. hominis* which consumes an extra amino acid alanine is also consumed. Some amino acids like methionine, tryptophan and leucine are left with some amount so we can feed less of these and reduce operating costs.

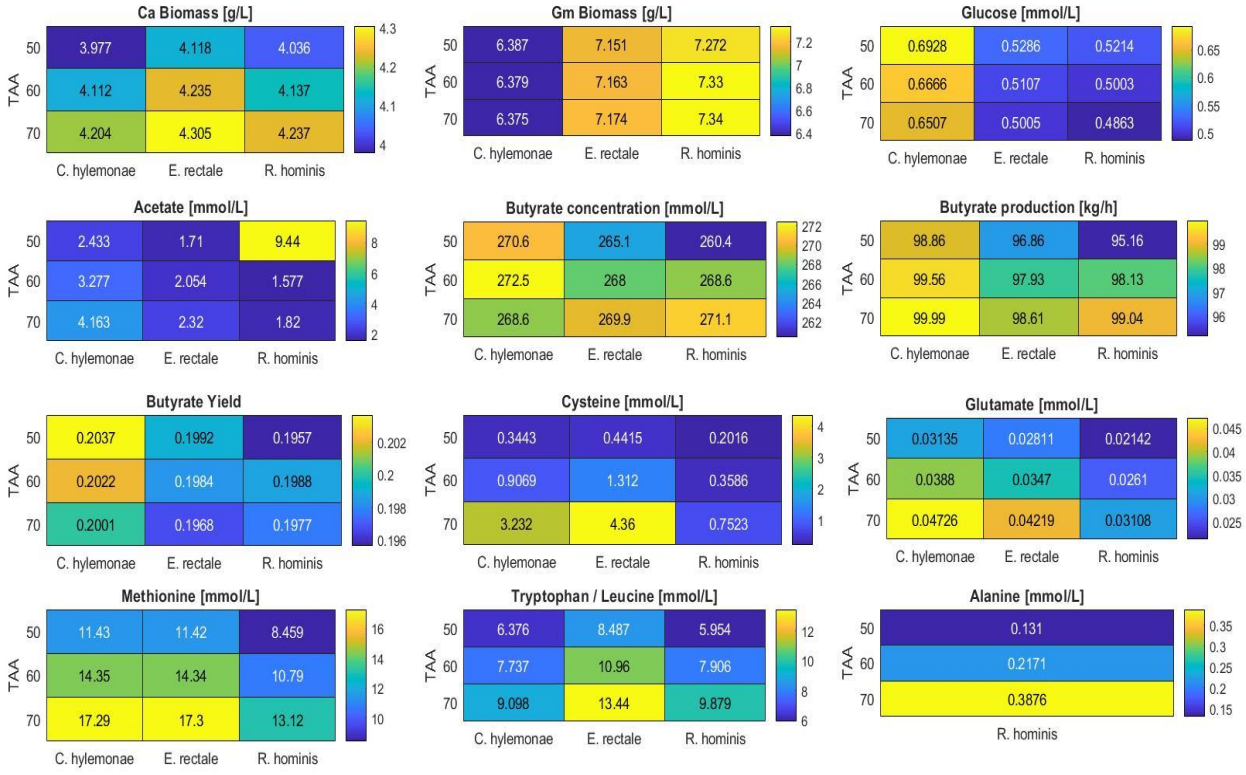

Figure 15: Steady state values of the liquid stream products exiting the column at the gas feed composition 50/30/20 ($CO/N_2/H_2$), and at varying total amino acids (TAA) in mmol/L. Ca is the acetogen *C. autoethanogenum*, Gm are the gut microbes *C. hylemonae*, *E. rectale* & *R. hominis*.

Acetate in each case (Fig. 15) is consumed almost fully which increases the butyrate production, just as we noticed the previous results at varying glucose (Fig. 13). Now, in the next steps we encountered some results while experimenting the column operating conditions.

4.4: Effect of Reactor Column Operating Conditions

The figure below is structured at varying initial bubble diameter in the system, with 1.5 mm as a base case value. With increase in bubble diameter, acetate converts the most but the butyrate production also drops from 1.5 mm to 2 mm bubble diameter because at larger bubble diameter the CO gas consumption is less which is not our objective. The butyrate production rate increases significantly about 57% more for the *C. hylemonae,* 75% more for the *E. rectale*, and 71% more for the *R. hominis*, from the range of 1 mm to 1.5 mm bubble diameter, but it decreases more than 10% thereafter.

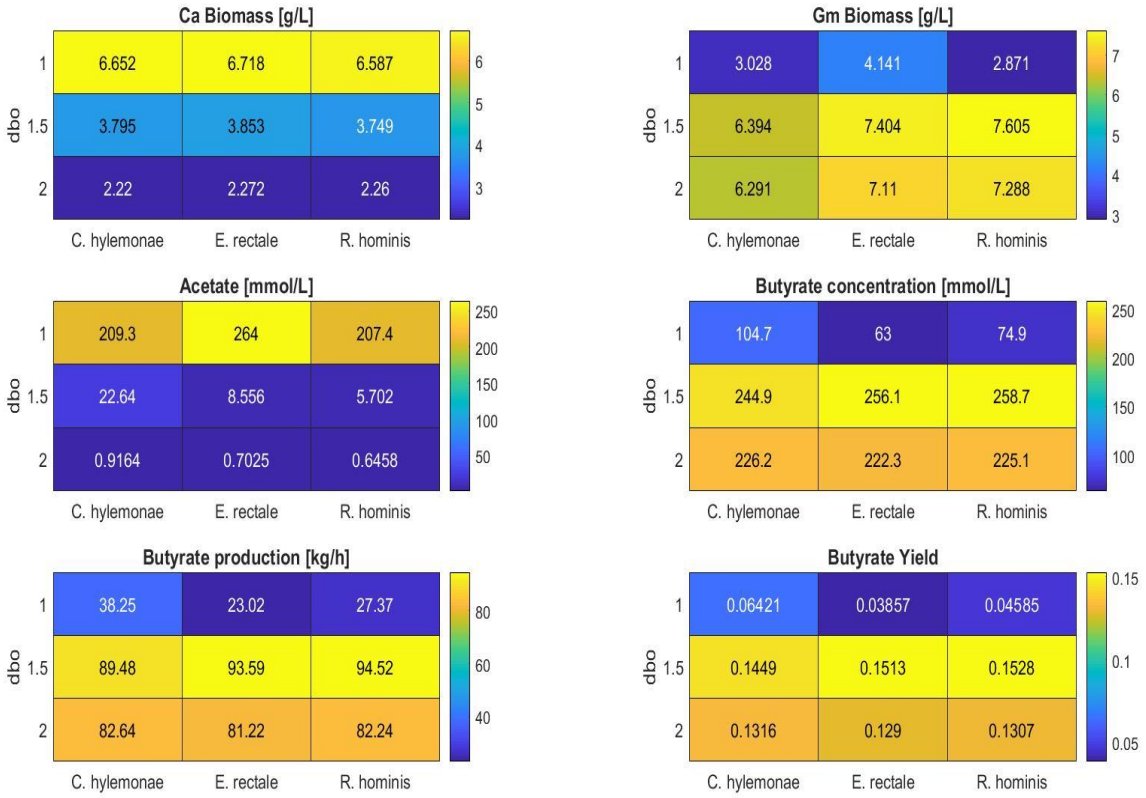

Figure 16: Steady state values of the liquid stream products exiting the column at the gas feed composition 70/30 (CO/N_2), and at varying bubble diameter (dbo) operating parameter in mm. Ca is the acetogen *C. autoethanogenum*, Gm are the gut microbes *C. hylemonae, E. rectale* & *R. hominis*.

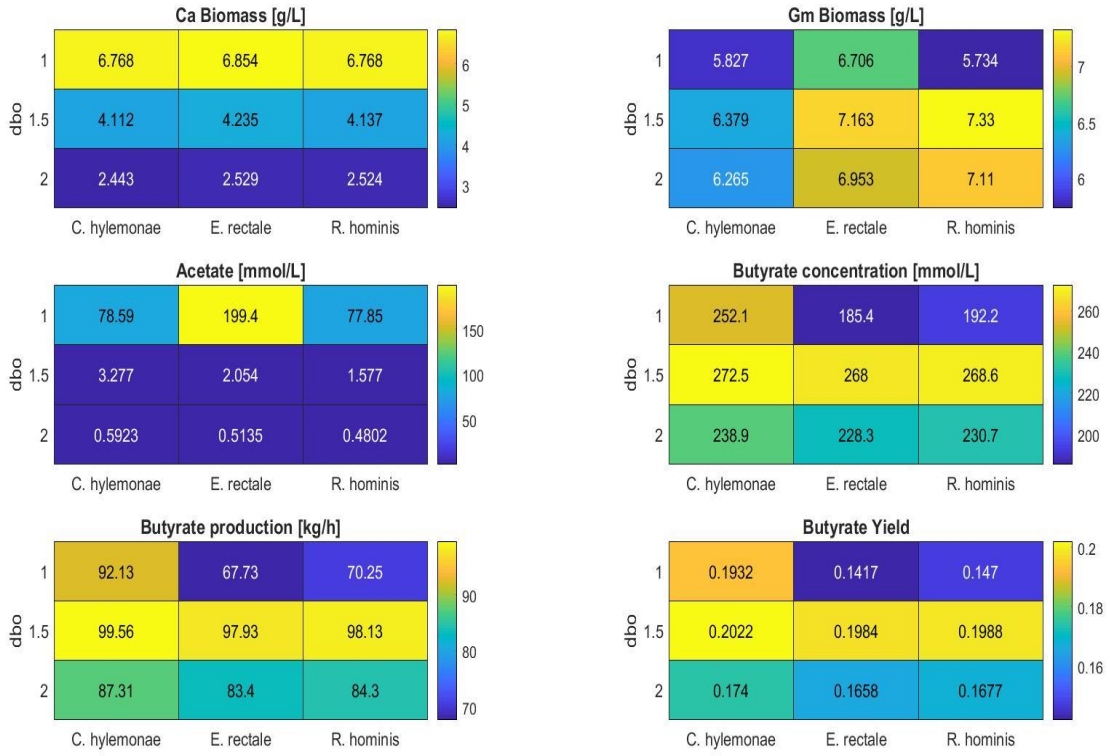

Figure 17: Steady state values of the liquid stream products exiting the column at the gas feed composition 50/30/20 ($CO/N_2/H_2$), and at varying bubble diameter (dbo) operating parameter in mm. Ca is the acetogen *C. autoethanogenum*, Gm are the gut microbes *C. hylemonae, E. rectale* & *R. hominis*.

Now, for the 1 mm bubble diameter operating condition if we consider hydrogen gas in the feed, then the butyrate production rate is on the higher end. The yield from the previous case (Fig. 16), was in the range of 3% to 6% for 1 mm bubble diameter, but now (Fig. 17) the yield is in the range of 14% to 19% which is significant for each microbe. However, acetate concentration at 1 mm is much more than at 1.5 mm and 2 mm condition but it can be fixed if we give more carbon source. The yield at 2 mm drops but not much which is redundant as our base case is 1.5 mm. It is further studied with the mass transfer coefficient operating conditions.

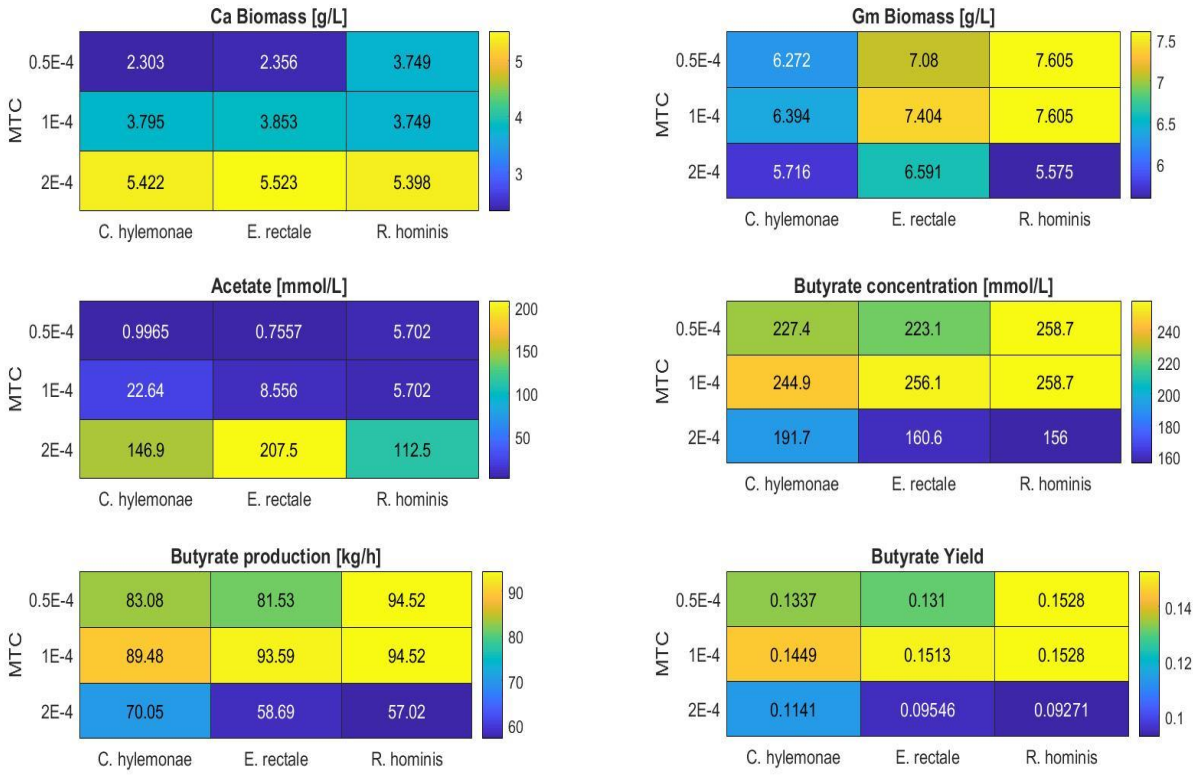

Figure 18: Steady state values of the liquid stream products exiting the column at the gas feed composition 70/30 (CO/N_2), and at varying mass transfer coefficient (MTC) operating parameter in m/s. Ca is the acetogen *C. autoethanogenum*, Gm are the gut microbes *C. hylemonae*, *E. rectale* & *R. hominis*.

These simulations (Fig. 18) were performed for different mass transfer coefficient in the range of 0.5E-4 m/s to 2E-4 m/s. *R. hominis* dominated these cases with higher butyrate production in each case and at the base case value the unconsumed acetate is comparatively less than the other two gut bacteria. Moreover, in our previous result where we studied the bubble diameter operating condition (Fig. 16), it showed similar results, but the largest mass transfer coefficient yields the lowest butyrate production since the acetate is not converted much in those case. The other gas stream composition in addition of hydrogen is not shown here (appendix Fig. A1) as the results did not show significant change.

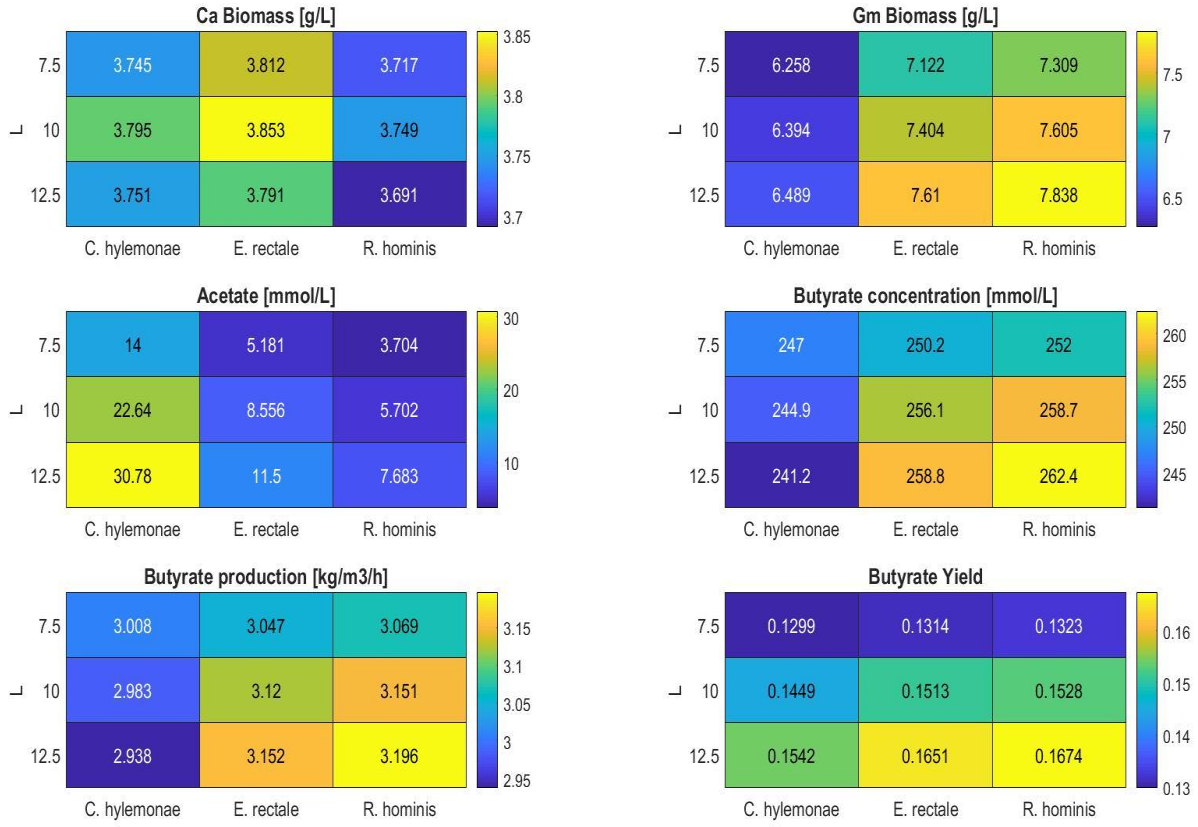

Figure 19: Steady state values of the liquid stream products exiting the column at the gas feed composition 70/30 (CO/N_2), and at varying column length (L) operating parameter in m. Ca is the acetogen *C. autoethanogenum*, Gm are the gut microbes *C. hylemonae, E. rectale* & *R. hominis*.

Column length is another a challenging part to discuss, the cost of a column or a bioreactor is decided with the column length and area. Higher the column length, more expensive is the column. We analyzed it for the column lengths 7.5m, 10m and for a 12.5m long length. In which initially we fixed it for a 7.5m column length but the yield was a main factor to consider at that point which brought us to test it for higher column length. At 7.5m length, the butyrate yield was in a range of 12% to 13% and we tried it to be something in a range of 15% to 16% or more than that. So we simulated it for higher column length and eventually the butyrate concentration increased marginally and the yield got fixed. The butyrate production in this case is monitored on volumetric production and

it showed that for a 10m column length, *E. rectale* and *R. hominis* dominated the *C. hylemonae*, but not in the case of hydrogen in the feed (appendix Fig. A2) with 20% yield in that case.

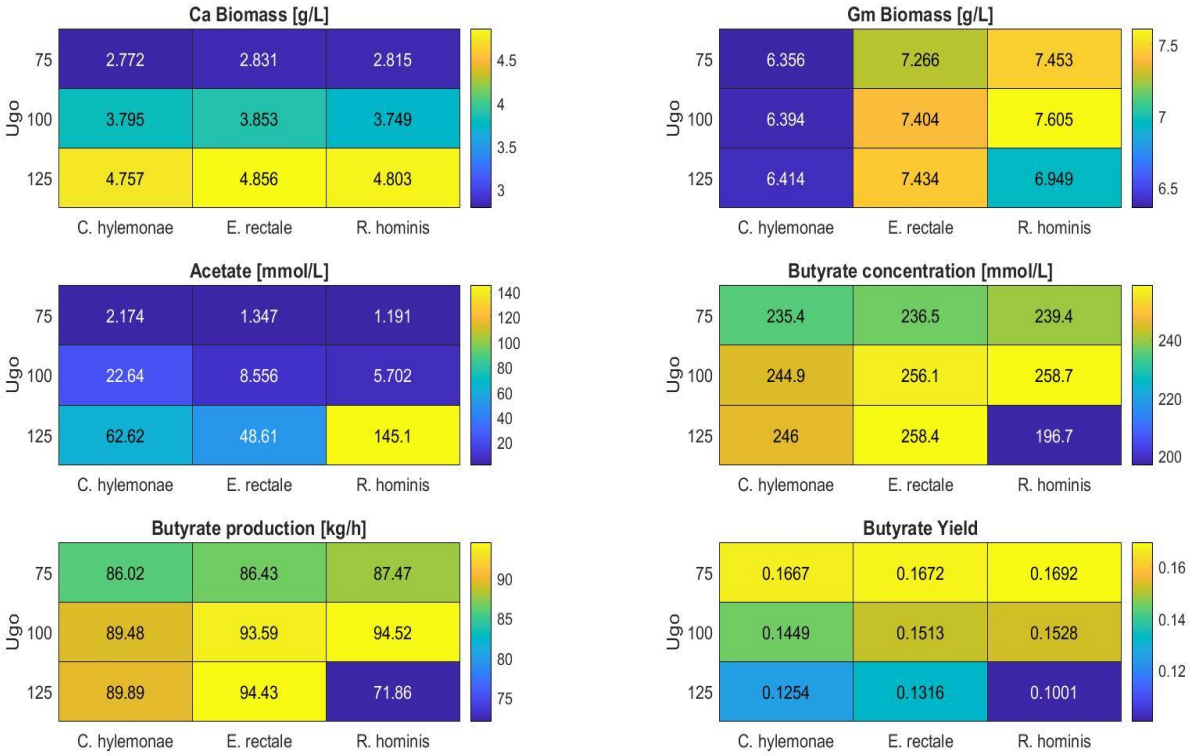

Figure 20: Steady state values of the liquid stream products exiting the column at the gas feed composition 70/30 (CO/N_2), and at varying superficial gas velocity (Ugo) operating parameter in m/h. Ca is the acetogen *C. autoethanogenum*, Gm are the gut microbes *C. hylemonae, E. rectale* & *R. hominis*.

Now, if I compare the result with varying superficial gas velocity, it showed that the column is not suitable for higher values above 100 m/hr because the acetate is not converted fully in those case. At 75 m/hr, the yield is higher than at 100 m/hr, because the CO gas conversion is more than at 75 m/hr. The butyrate production on the other hand for 100 m/hr are higher and since our aim is to convert CO to butyrate so we adjusted the gas velocity to be 100 m/hr as our base case value because it produced more than 7% butyrate for *E. rectale* and *R. hominis*.

CHAPTER 5

CONCLUSION

In summary, I have successfully modeled the bubble column reactor for the combination of the acetogen *Clostridium autoethanogenum* with the gut microbes *Clostridium hylemonae*, *Eubacterium rectale,* and *Roseburia hominis*. This work was emphasized more on to maximize the butyrate or the biochemical production by taking the essential nutrients, carbon sources and minimum medium requirement into the account. I performed the flux balance analysis (FBA), to examine the growth and metabolites secretion of each bacteria and further performed the dynamic flux balance analysis (DFBA) to check the behavior in a column spatially. I further studied and performed the sensitivity analysis to monitor the optimization of carbon sources like glucose and amino acids. I also investigated the performance of the column at varying operating conditions which showed some promising results. I predicted the following trends for the better performance to maximize the butyrate production considering the operating parameters at base values.

- *E. rectale* and *R. hominis* are promising because of their growth rate and the add on advantage of H_2 production while performing the flux balance analysis.
- In terms of butyrate production at 70/30 (CO/N_2), *R. hominis* design performed better at our base value dilution rate of 0.14 h^{-1}, and in presence of H_2 in the gas feed 50/20/30 ($CO/H_2/ N_2$), *C. hylemonae* yielded the highest butyrate production rate with 99.56 kg/hr.
- *C. hylemonae* demands more glucose to convert acetate to butyrate with 70/30 (CO/N_2) feed composition, but it is favorable with the gas feed composition 50/20/30 ($CO/H_2/N_2$).

- *C. hylemonae* design performs better at lower value of 50 mmol/L total amino acid at both gas feed combinations.
- *R. hominis* dominated the other two bacteria at lower mass transfer coefficient accounting 13% more butyrate.
- *E. rectale* and *R. hominis* were superior for different combination of column length with gas feed 70/30 (CO/N_2), but *C. hylemonae* is a better option if H_2 is present in the feed.
- With varying superficial gas velocity, the *E. rectale* design dominated for each case with better yield.

R. hominis requires an addition of amino acid which is alanine and it would cost more so we can say it may not be the best option or microbe to produce butyrate at minimum cost. It didn't perform better at lower bubble diameter operating condition when H_2 was introduced in the feed, and it is unable to produce much butyrate at 50 mmol/L of total amino acids which is below our base case value of 60 mmol/L unlike *C. hylemonae*. However, there is a trade-off between the *C. hylemonae* and *E. rectale*, in some case I found *E. rectale* to be dominating and vice versa. The *C. hylemonae* requires more amount of glucose to convert the unconsumed acetate which means more resource would require, and on the other hand if we follow the *E. rectale* model, FBA results showed that it has a tendency to produce hydrogen (H_2) which is an addition to a system.

CHAPTER 6

FUTURE WORK

Further enhancement in the model would be to test experimentally for the continuous stirred tank bioreactor (CSTBR) with each combination which we designed in this work, but bubble column bioreactor would be preferred for a large scale production. We can also estimate the parameters for a monoculture experiments from CSTBR which can mainly study the gas uptake kinetics by monitoring the growth rate of the bacterium with some combination of uptake values.

It would be interesting to try the adjustment of ATP maintenance to match the growth rates and further constrain the genome scale metabolic models to byproduct synthesis. This can be tracked by performing the flux balance analysis for a particular bacterium.

We can also estimate or optimize the amino acid requirement for each bacterium individually by allowing separate design equations for the total amino acids.

APPENDICES

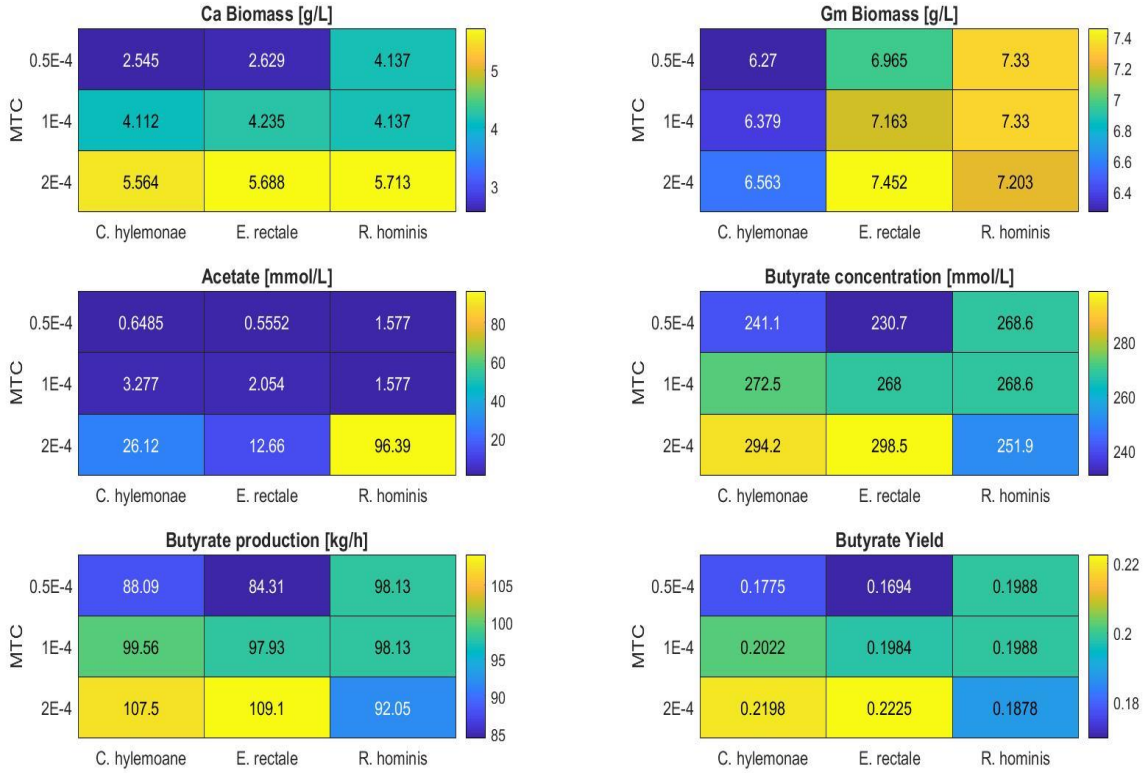

Figure A1: Steady state values of the liquid stream products exiting the column at the gas feed composition 50/20/30 ($CO/H_2/N_2$), and at varying mass transfer coefficient (MTC) operating parameter in m/s. Ca is the acetogen *C. autoethanogenum*, Gm are the gut microbes *C. hylemonae, E. rectale* & *R. hominis*.

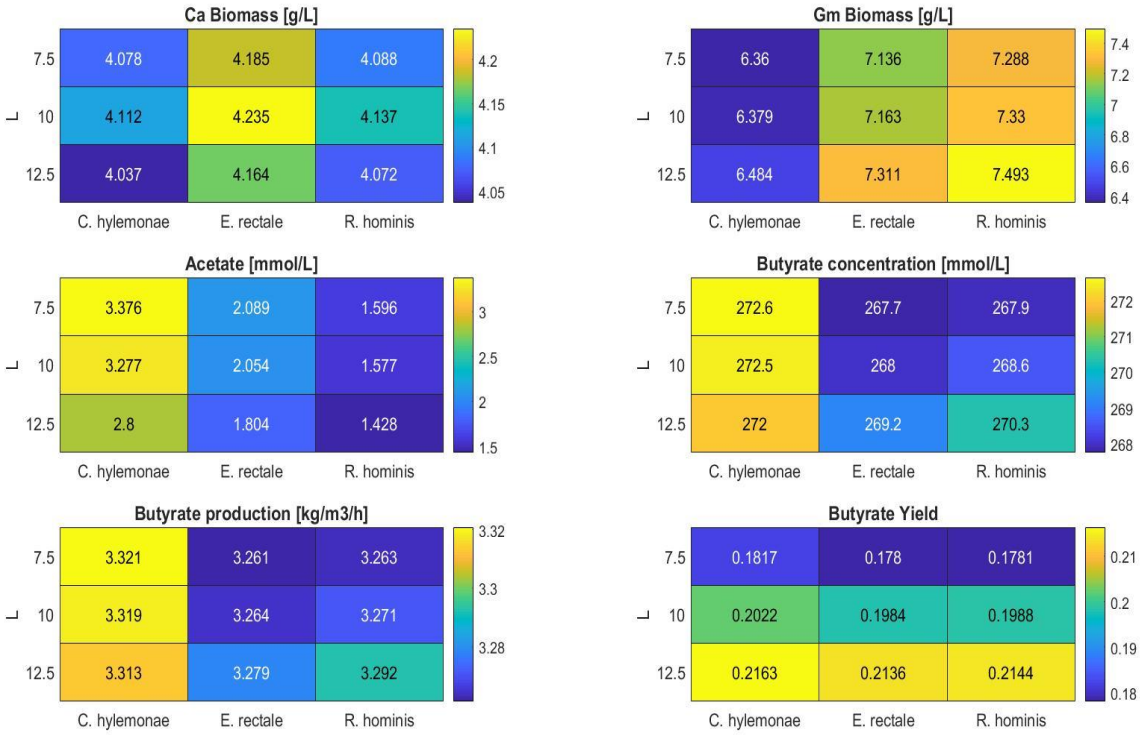

Figure A2: Steady state values of the liquid stream products exiting the column at the gas feed composition 50/20/30 ($CO/H_2/N_2$), and at varying column length (L) operating parameter in m. Ca is the acetogen *C. autoethanogenum*, Gm are the gut microbes *C. hylemonae*, *E. rectale* & *R. hominis*.

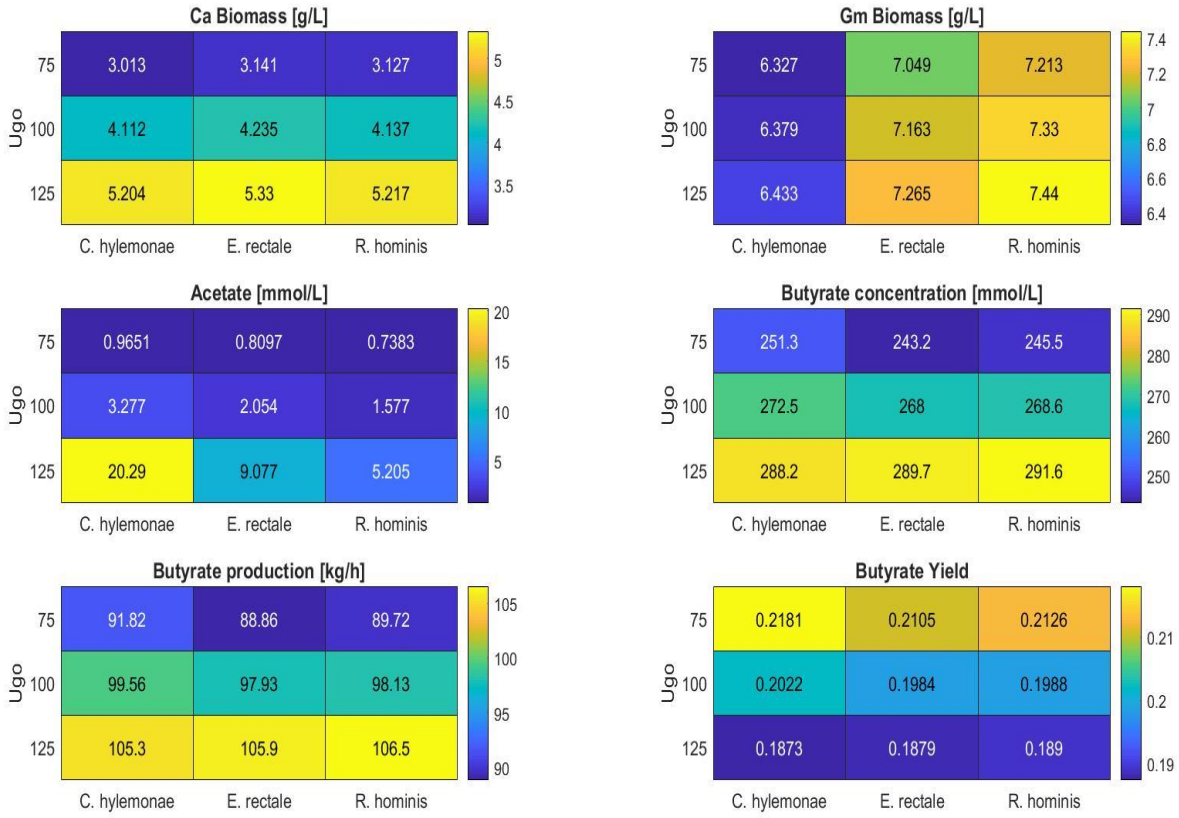

Figure A3: Steady state values of the liquid stream products exiting the column at the gas feed composition 50/20/30 ($CO/H_2/N_2$), and at varying superficial gas velocity (Ugo) operating parameter in m/h. Ca is the acetogen *C. autoethanogenum*, Gm are the gut microbes *C. hylemonae*, *E. rectale* & *R. hominis*.

REFERENCES

[1] Vasudevan PT, Gagnon MD, Briggs MS. Environmentally sustainable biofuels – The case for biodiesel, biobutanol and cellulosic ethanol. In: Singh OV, Harvey SP, editors. Sustainable Biotechnology: Sources of Renewable Energy: Springer Science+Business Media B.V.; 2010. p. 43-62.

[2] Appenzeller T. The end of cheap oil. National Geographic Magazine. 2004.

[3] European_Union. Directive 2009/28/EC of the European Parliament and of the Council of 23 April 2009 on the promotion of the use of energy from renewable sources and amending and subsequently repealing Directives 2001/77/EC and 2003/30/EC. 2009.

[4] REN21. Renewables 2011 Global Status Report. Paris: REN21, 2011.

[5] Demirbas A. Political, economic and environmental impacts of biofuels: A review. Applied Energy. 2009 Nov;86: S108-S17. PubMed PMID: WOS:000271170300013.

[6] Abubackar, H. N., Veiga, M. C., & Kennes, C. (2011). Biological conversion of carbon monoxide: Rich syngas or waste gases to bioethanol. Biofuels, Bioproducts and Biorefining, 5(1), 93–114.

[7] Abubackar, H. N., Veiga, M. C., & Kennes, C. (2015). Carbon monoxide fermentation to ethanol by *Clostridium autoethanogenum* in a bioreactor with no accumulation of acetic acid. Bioresource Technology, 186, 122–127.

[8] Datar, R. P., Shenkman, R. M., Cateni, B. G., Huhnke, R. L., & Lewis, R. S. (2004). Fermentation of biomass-generated producer gas to ethanol. Biotechnology and Bioengineering, 86(5), 587–594.

[9] McKendry, P. Energy production from biomass (Part 3): Gasification technologies. Bioresour. Technol. 2002, 83, 55–63.

[10] Kirkels, A.F.; Verbong, G.P.J. Biomass gasification: Still promising? A 30-year global overview. Renew. Sustain. Energy Rev. 2011, 15, 471–481.

[11] Matsumura, Y.; Minowa, T.; Potic, B.; Kersten, S.; Prins, W.; Vanswaaij, W.; Vandebeld, B.; Elliott, D.; Neuenschwander, G.; Kruse, A. Biomass gasification in near- and super-critical water: Status and prospects. Biomass Bioenergy 2005, 29, 269–292.

[12] Babu, S. Thermal gasification of biomass technology developments: end of task report for 1992 to 1994. Biomass Bioenergy 1995, 9, 271–285.

[13] Xu, D.; Tree, D.R.; Lewis, R.S. The effects of syngas impurities on syngas fermentation to liquid fuels. Biomass Bioenergy 2011, 35, 2690–2696.

[14] Kopke, M., Held, C., Hujer, S., Liesegang, H., Wiezer, A., Wollherr, A., Durre, P. (2010). *Clostridium ljungdahlii* represents a microbial production platform based on syngas. Proceedings of the National Academy of Sciences of the United States of America, 107(29), 13087–13092.

[15] Phillips, J. R., Klasson, K. T., Clausen, E. C., & Gaddy, J. L. (1993). Biological production of ethanol from coal synthesis gas. Applied Biochemistry and Biotechnology, 39(1), 559–571.

[16] Younesi, H., Najafpour, G., & Mohamed, A. R. (2005). Ethanol and acetate production from synthesis gas via fermentation processes using anaerobic bacterium, *Clostridium ljungdahlii*. Biochemical Engineering Journal, 27(2), 110–119.

[17] Guo, Y., Xu, J., Zhang, Y., Xu, H., Yuan, Z., & Li, D. (2010). Medium optimization for ethanol production with *Clostridium autoethanogenum* with carbon monoxide as sole carbon source. Bioresource Technology, 101(22), 8784–8789.

[18] Liew, F., Henstra, A. M., Köpke, M., Winzer, K., Simpson, S. D., & Minton, N. P. (2017). Metabolic engineering of *Clostridium autoethanogenum* for selective alcohol production. Metabolic Engineering, 40, 104–114.

[19] Cotter, J. L., Chinn, M. S., & Grunden, A. M. (2009a). Ethanol and acetate production by *Clostridium ljungdahlii* and *Clostridium autoethanogenum* using resting cells. Bioprocess and Biosystems Engineering, 32(3), 369–380.

[20] Cotter, J. L., Chinn, M. S., & Grunden, A. M. (2009b). Influence of process parameters on growth of *Clostridium ljungdahlii* and *Clostridium autoethanogenum* on synthesis gas. Enzyme and Microbial Technology, 44(5), 281–288.

[21] Heijstra, B. D., Kern, E., Koepke, M., Segovia, S., & Liew, F. (2013). Novel bacteria and methods of use thereof. Google Patents US20130217096A1.

[22] Heijstra, B. D., Kern, E., Koepke, M., Segovia, S., & Liew, F. M. (2016). Novel bacteria and methods of use thereof. Google Patents US20160017276A1.

[23] Simpson, S. D., Forster, R. L. S., Tran, P. L., Rowe, M. J., & Warner, I. L. (2014). Bacteria and methods of use thereof. Google Patents US8852918B2.

[24] Chen, J., Daniell, J., Griffin, D., Li, X., & Henson, M. A. (2018). Experimental testing of a spatiotemporal metabolic model for carbon monoxide fermentation with *Clostridium autoethanogenum*. Biochemical Engineering Journal, 129, 64-73.

[25] Chen, J., Gomez, J. A., Höffner, K., Barton, P. I., & Henson, M. A. (2015). Metabolic modeling of synthesis gas fermentation in bubble column reactors. Biotechnology for biofuels, 8(1), 89.

[26] Chen, J., Gomez, J. A., Höffner, K., Phalak, P., Barton, P. I., & Henson, M. A. (2016). Spatiotemporal modeling of microbial metabolism. BMC systems biology, 10(1), 21.

[27] Chen, J., & Henson, M. A. (2016). In silico metabolic engineering of *Clostridium ljungdahlii* for synthesis gas fermentation. Metabolic engineering, 38, 389-400.

[28] Nagarajan, H., Sahin, M., Nogales, J., Latif, H., Lovley, D. R., Ebrahim, A., & Zengler, K. (2013). Characterizing acetogenic metabolism using a genome-scale metabolic reconstruction of *Clostridium ljungdahlii*. Microbial cell factories, 12(1), 118.

[29] Millies, M., & Mewes, D. (1999). Interfacial area density in bubbly flow. Chemical Engineering and Processing: Process Intensification, 38(4), 307-319.

[30] Schäfer, R., Merten, C., & Eigenberger, G. (2002). Bubble size distributions in a bubble column reactor under industrial conditions. Experimental Thermal and Fluid Science, 26(6), 595-604.

[31] Shaikh, A., & Al-Dahhan, M. H. (2007). A review on flow regime transition in bubble columns. International Journal of Chemical Reactor Engineering, 5(1).

[32] Stegeman, D., Knop, P., Wijnands, A., & Westerterp, K. (1996). Interfacial area and gas holdup in a bubble column reactor at elevated pressures. Industrial & engineering chemistry research, 35(11), 3842-3847.

[33] X. Li, D. Griffin, X. Li, M.A. Henson, Incorporating hydrodynamics into spatiotemporal metabolic models of bubble column gas fermentation, Biotechnol. Bioeng. 116 (1) (2019) 28–40.

[34] Li, X. and M.A. Henson, Metabolic Modeling of Bacterial Co-Culture Systems Predicts Enhanced Carbon Monoxide-to-Butyrate Conversion Compared to Monoculture Systems. Biochemical Engineering Journal, 2019. 151: p. 107338.

[35] Saeed Shoaie, Fredrik Karlsson, Adil Mardinoglu, Intawat Nookaew, Sergio Bordel & Jens Nielsen, Understanding the interactions between bacteria in the human gut through metabolic modeling. Sci. Rep. 3, 2532; DOI:10.1038/srep02532 (2013).

[36] Zuber, N., & Findlay, J. A. (1965). Average volumetric concentration in two-phase flow systems. Journal of Heat Transfer, 87(4), 453–468.

[37] Clark, N. N., Van Egmond, J. W., & Nebiolo, E. P. (1990). The drift-flux model applied to bubble columns and low velocity flows. International Journal of Multiphase Flow, 16(2), 261–279.

[38] Wallis, G. B. (1969). One-dimensional two-phase flow. NewYork:McGraw-Hill.

[39] Peebles, F. N. (1953). Studies on the motion of gas bubbles in liquids. Chemical Engineering Progress, 49, 88–97.

[40] Akita, K., & Yoshida, F. (1974). Bubble size, interfacial area, and liquid- phase mass transfer coefficient in bubble columns. Industrial & Engineering Chemistry Process Design and Development, 13(1), 84–91.

[41] Maceiras, R., Álvarez, E., & Cancela, M. A. (2010). Experimental interfacial area measurements in a bubble column. Chemical Engineering Journal, 163(3), 331–336.

[42] Van't Riet, K., & Tramper, J. (1991). Basic bioreactor design. CRC Press.

[43] Kantarci, N., Borak, F., & Ulgen, K. O. (2005). Bubble column reactors. Process Biochemistry, 40(7), 2263–2283.

[44] Abrini, J., Naveau, H., & Nyns, E. -J. (1994). *Clostridium autoethanogenum*, sp. nov., an anaerobic bacterium that produces ethanol from carbon monoxide. Archives of Microbiology, 161(4), 345–351.

[45] J. Daniell, M. Köpke, S.D. Simpson, Commercial biomass syngas fermentation, Energies 5 (12) (2012) 5372–5417.

[46] M. Mohammadi, A.R. Mohamed, G.D. Najafpour, H. Younesi, M.H. Uzir, Kinetic studies on fermentative production of biofuel from synthesis gas using *Clostridium ljungdahlii*, Scientific World J. 2014 (2014).

[47] K. Valgepea, R.S.P. Lemgruber, T. Abdalla, S. Binos, N. Takemori, A. Takemori, Y. Tanaka, R. Tappel, M. Köpke, S.D. Simpson, H_2 drives metabolic rearrangements in gas-fermenting *Clostridium autoethanogenum*, Biotechnol. Biofuels 11 (1) (2018) 55.

[48] Kapic A, Jones ST, Heindel TJ. Carbon monoxide mass transfer in a syngas mixture. Industrial & Engineering Chemistry Research. 2006 Dec; 45(26):9150-5. PubMed PMID: WOS:000242786200049.

[49] Mohammadi M, Najafpour GD, Younesi F, Lahijani P, Uzir MH, Mohamed AR. Bioconversion of synthesis gas to second generation biofuels: A review. Renewable & Sustainable Energy Reviews. 2011 Dec;15(9):4255-73. PubMed PMID: WOS: 000298764400005.

[50] Munasinghe PC, Khanal SK. Biomass-derived syngas fermentation into biofuels: Opportunities and challenges. Bioresour Technol. 2010;101(13):5013-22.

[51] Bredwell MD, Srivastava P, Worden RM. Reactor design issues for synthesis-gas fermentations. Biotechnology Progress. 1999 Sep-Oct;15(5):834-44. PubMed PMID: WOS:000082936200007.

[52] Abubackar HN, Veiga MC, Kennes C, Coruña L. Biological conversion of carbon monoxide: rich syngas or waste gases to bioethanol. Biofuels, Bioproducts & Biorefining. 2011:93-114.

[53] O. Levenspiel, The Monod equation: a revisit and a generalization to product inhibition situations, Biotechnol. Bioeng. 22 (8) (1980) 1671–1687.

[54] Noronha et al., "The Virtual Metabolic Human database: integrating human and gut microbiome metabolism with nutrition and disease", Nucleic Acids Research (2018); https://academic.oup.com/nar/advance-article/doi/10.1093/nar/gky992/5146204

[55] Gomez, J. A., Höffner, K., & Barton, P. I. (2014). DFBAlab: A fast and reliable MATLAB code for dynamic flux balance analysis. BMC Bioinformatics, 15(1), 409.

[56] Höffner, K., Harwood, S. M., & Barton, P. I. (2013). A reliable simulator for dynamic flux balance analysis. Biotechnology and Bioengineering, 110 (3), 792–802.

[57] Michael Q. Wang, “Energy and greenhouse gas emission effects of corn and cellulosic ethanol with technology improvements and land use changes,” Biomass and Bioenergy, 35, no 5, (May 2011), pp. 1885-1896.

[58] Reed JL & Palsson BO (2003) Thirteen years of building constraint-based in silico models of Escherichia coli. J Bacteriol 185: 2692–2699.

[59] Maxime Durot, Pierre-Yves Bourguignon, Vincent Schachter, Genome-scale models of bacterial metabolism: reconstruction and applications, FEMS Microbiology Reviews, Volume 33, Issue 1, January 2009, Pages 164–190, https://doi.org/10.1111/j.1574-6976.2008.00146.x

[60] Dwidar, Mohammed & Park, Jae-Yeon & Mitchell, Robert & Sang, Byoung-In. (2012). The Future of Butyric Acid in Industry. The Scientific World Journal. 2012. 471417. 10.1100/2012/471417.

[61] S.W. Ragsdale, E. Pierce, Acetogenesis and the Wood–Ljungdahl pathway of CO_2 fixation, Biochimica et Biophysica Acta (BBA)-Proteins Proteomics 1784 (12) (2008) 1873–1898.

[62] Brown, Robert C. (2003). Biorenewable resources: engineering new products from agriculture. Ames, Iowa: Iowa State Press. ISBN 0-8138-2263-7.

[63] Worden, R.M., Bredwell, M.D., and Grethlein, A.J. (1997). Engineering issues in synthesis gas fermentations, Fuels and Chemicals from Biomass. Washington, DC: American Chemical Society, 321-335.

[64] Abubackar, H.N.; Veiga, M. C.; Kennes, C. (2011). "Biological conversion of carbon monoxide: rich syngas or waste gases to bioethanol" Biofuels, Bioproducts and Biorefining. 5 (1): 93–114. doi:10.1002/bbb.256.